Volume 4

Chapter 7

https://doi.org/10.32685/pub.esp.38.2019.07
Published online 27 November 2020

Geological Evolution of the Nevado del Ruiz Volcanic Complex

Julián Andrés CEBALLOS–HERNÁNDEZ[1]*, Lilly Maritza MARTÍNEZ–TABARES[2], Luis Gerónimo VALENCIA–RAMÍREZ[3], Bernardo Alonso PULGARÍN–ALZATE[4]*, Ana María CORREA–TAMAYO[5], and Blanca Liliana NARVÁEZ–MARULANDA[6]

1 jaceballos@sgc.gov.co
Servicio Geológico Colombiano
Observatorio Vulcanológico y Sismológico de Manizales
Avenida 12 de octubre n.° 15–47
Manizales, Colombia

2 lmmartinez@sgc.gov.co
Servicio Geológico Colombiano
Observatorio Vulcanológico y Sismológico de Manizales
Avenida 12 de octubre n.° 15–47
Manizales, Colombia

3 ljvalencia@sgc.gov.co
Servicio Geológico Colombiano
Observatorio Vulcanológico y Sismológico de Manizales
Avenida 12 de octubre n.° 15–47
Manizales, Colombia

4 bpulgarin@sgc.gov.co
Servicio Geológico Colombiano
Dirección de Geociencias Básicas
Observatorio Vulcanológico y Sismológico de Popayán
Calle 5b n.° 2–14, Loma Cartagena
Popayán, Colombia

5 acorrea@sgc.gov.co
Servicio Geológico Colombiano
Dirección de Geociencias Básicas
Diagonal 53 n.° 34–53
Bogotá, Colombia

6 liliananarvaezco@yahoo.com
Bonn Universität and United Nations University
Bonn, Germany

* Corresponding author

Abstract New results based on modern methods of volcanic mapping and stratigraphy used in the area domain of the Nevado del Ruiz Volcano, combined with the review of previous studies and the contribution of new geochronological, petrographic, and geochemical data, are presented to define the Nevado del Ruiz Volcanic Complex. The geological evolution of this complex consists of four eruptive periods that were characterized by the construction and destruction of volcanic edifices and deposits associated with effusive products (lava flows and lava domes), primary volcaniclastic deposits (pyroclastic density currents and pyroclastic falls), secondary volcaniclastic deposits (lahars and debris avalanches), and glacial and fluvial deposits. The Pre–Ruiz eruptive period was dominated by effusive volcanism and the construction of the "Ancestral Ruiz" volcano; known ages range from 1.8 to 0.97 Ma. The First eruptive period Ruiz corresponded to the construction of the "Older Ruiz" volcano and it was defined by effusive volcanism that started less than 0.97 Ma; the construction of La Olleta Volcano began at the end of this eruptive period at approximately 107 ka, and the destructive period of the "Older Ruiz" volcano occurred at approximately 95 ka, leading to the formation of a caldera. The Intermediate eruptive period Ruiz corresponded to the origin of the volcanoes Piraña and Nereidas and to the continuation of the construction of La Olleta Volcano, as well as the occurrence of other minor eruptive centers. In the Second eruptive period Ruiz the Nevado del Ruiz Volcano was formed; this eruptive period began 66 ka ago. During the last 13 ka, explosive activity has been predominant, at least fourteen pulses and eruptive phases have occurred. The present study provides new knowledge towards understanding the eruptive history of the Nevado del Ruiz Volcanic Complex.

Keywords: *Nevado del Ruiz Volcanic Complex, Nevado del Ruiz Volcano, geological evolution, eruptive periods.*

Resumen Nuevos resultados basados en técnicas modernas de cartografía y estratigrafía de volcanes en el área de dominio del Volcán Nevado del Ruiz, combinados con la revisión de estudios previos y nuevos datos geocronológicos, petrográficos y geoquímicos, se presentan para definir el Complejo Volcánico Nevado del Ruiz. La evolución geológica de este complejo consiste de cuatro períodos eruptivos que se caracterizaron por la construcción y destrucción de edificios volcánicos y depósitos asociados

Citation: Ceballos–Hernández, J.A., Martínez–Tabares, L.M., Valencia–Ramírez, L.G., Pulgarín–Alzate, B.A., Correa–Tamayo, A.M. & Narváez–Marulanda, B.L. 2020. Geological evolution of the Nevado del Ruiz Volcanic Complex. In: Gómez, J. & Pinilla–Pachon, A.O. (editors), The Geology of Colombia, Volume 4 Quaternary. Servicio Geológico Colombiano, Publicaciones Geológicas Especiales 38, p. 267–296. Bogotá. https://doi.org/10.32685/pub.esp.38.2019.07

con productos efusivos (flujos de lava y domos de lava), depósitos volcanoclásticos primarios (corrientes de densidad piroclástica y caídas piroclásticas), depósitos volcanoclásticos secundarios (lahares y avalanchas de escombros) y depósitos glaciares y fluviales. El período eruptivo Pre–Ruiz estuvo dominado por vulcanismo efusivo y la construcción del volcán "Ruiz Ancestral"; las edades conocidas están entre 1,8 y 0,97 Ma. El primer período eruptivo Ruiz correspondió a la construcción del volcán "Ruiz Antiguo", que estuvo definido por un vulcanismo efusivo que comenzó hace menos de 0,97 Ma; al final de este período eruptivo, hace 107 ka aproximadamente, inició la construcción del Volcán La Olleta; la época destructiva del volcán "Ruiz Antiguo" ocurrió hace 95 ka aproximadamente, y condujo a la formación de una caldera. El período eruptivo Ruiz intermedio correspondió al origen de los volcanes Piraña y Nereidas y a la continuación de la construcción del Volcán La Olleta, así como la ocurrencia de otros centros eruptivos menores. En el segundo período eruptivo Ruiz se formó el actual Volcán Nevado del Ruiz; este período eruptivo comenzó hace 66 ka. Durante los últimos 13 ka ha predominado la actividad explosiva, al menos catorce pulsos y fases eruptivas han ocurrido. El presente estudio provee nuevo conocimiento para el entendimiento de la historia eruptiva del Complejo Volcánico Nevado del Ruiz.

Palabras clave: *Complejo Volcánico Nevado del Ruiz, Volcán Nevado del Ruiz, evolución geológica, períodos eruptivos.*

1. Introduction

The Nevado del Ruiz Volcanic Complex (NRVC) is defined as a series of volcanic structures and deposits genetically related to the development of the Nevado del Ruiz Volcano (NRV). The NRV is an active composite volcano that peaks at 5321 masl and is crowned by the Arenas Crater (approximately 750 m in diameter and 200 m in depth). The NRV is located (Figure 1) in the middle section of the Central Cordillera of Colombia (4° 53' 43'' N, 75° 19' 21'' W), between the Caldas and Tolima Departments, and approximately 140 km NW of Bogotá, capital of Colombia, and 28 km SE of Manizales, Caldas. It currently has a glacial cover of 9.3 km^2. The phreatomagmatic eruption on 13 November 1985, which had a Volcanic Explosivity Index (VEI) of 3, generated lahars (Calvache, 1990; Pierson et al., 1990) that caused more than 25 000 deaths in the municipalities of Armero, Villamaría, and Chinchiná. The NRV has been monitored since 1985 by the Servicio Geológico Colombiano (SGC) at its Observatorio Vulcanológico y Sismológico de Manizales (OVSM).

The NRV, also known as *Kumanday* or *Tama* during the Quimbaya civilization, has been included with other nearby volcanoes in the Ruiz–Tolima Volcanic Complex (Herd, 1974), the Ruiz–Tolima Volcanic Massif (Thouret, 1988), or the Cerro Bravo–Machín Volcanic Complex (Méndez & Patiño, 1994). Several authors have studied the general stratigraphy of the NRV, primarily Herd (1974), (Central Hidroeléctrica de Caldas S.A., 1983), Schaefer (1995), Thouret (1988), and Thouret et al. (1985, 1990). In the present study, the terms "Ancestral Ruiz" and "Older Ruiz", based on Thouret et al. (1990), were adopted to define which volcanic edifices were involved in the evolution of the NRVC.

The study area covers 3600 km^2 and includes parts of the Tolima and Caldas Departments in the central zone of the Central Cordillera between the Cauca (to the W) and Magdalena (to the E) River valleys of the NRVC. The proximal zone of the complex is located near the NRV. The distal zone corresponds to the low sections of the Gualí; Azufrado; Lagunilla; Recio, Tolima; and Chinchiná and Claro, Caldas River Basins (Figure 2).

Regarding the study location, scope, or geoscientific discipline addressed, the NRV has been the object of numerous specific studies. However, until Thouret et al. (1990), no comprehensive study had been conducted to understand the eruptive history of the volcanic complex, nor the volcanic facies architecture and its interaction with the terrestrial environment. Furthermore, in recent years, key changes to the understanding of basic concepts in volcanology have occurred and new internationally validated volcanic mapping and stratigraphy methods have been introduced (e.g., Fisher & Schmincke, 1984; Groppelli & Viereck–Goette, 2010; Lucchi, 2013; Martí et al., 2018; Murcia et al., 2013; Sigurdsson et al., 2000). The present study gathers and summarizes the results from integrated research conducted in recent years by the Grupo de Geología de Volcanes of the SGC on the geology, stratigraphy, and eruptive history of the NRVC (Martínez et al., 2014).

2. Materials and Methods

The present study is based on a detailed stratigraphic survey of volcanic deposits at a 1:25 000 map scale, in addition to a morphogenetic analysis from Advanced Spaceborne Thermal Emission and Reflection Radiometer (ASTER), Rapid Eye and LandSat satellite images, and uninhabited aerial vehicle

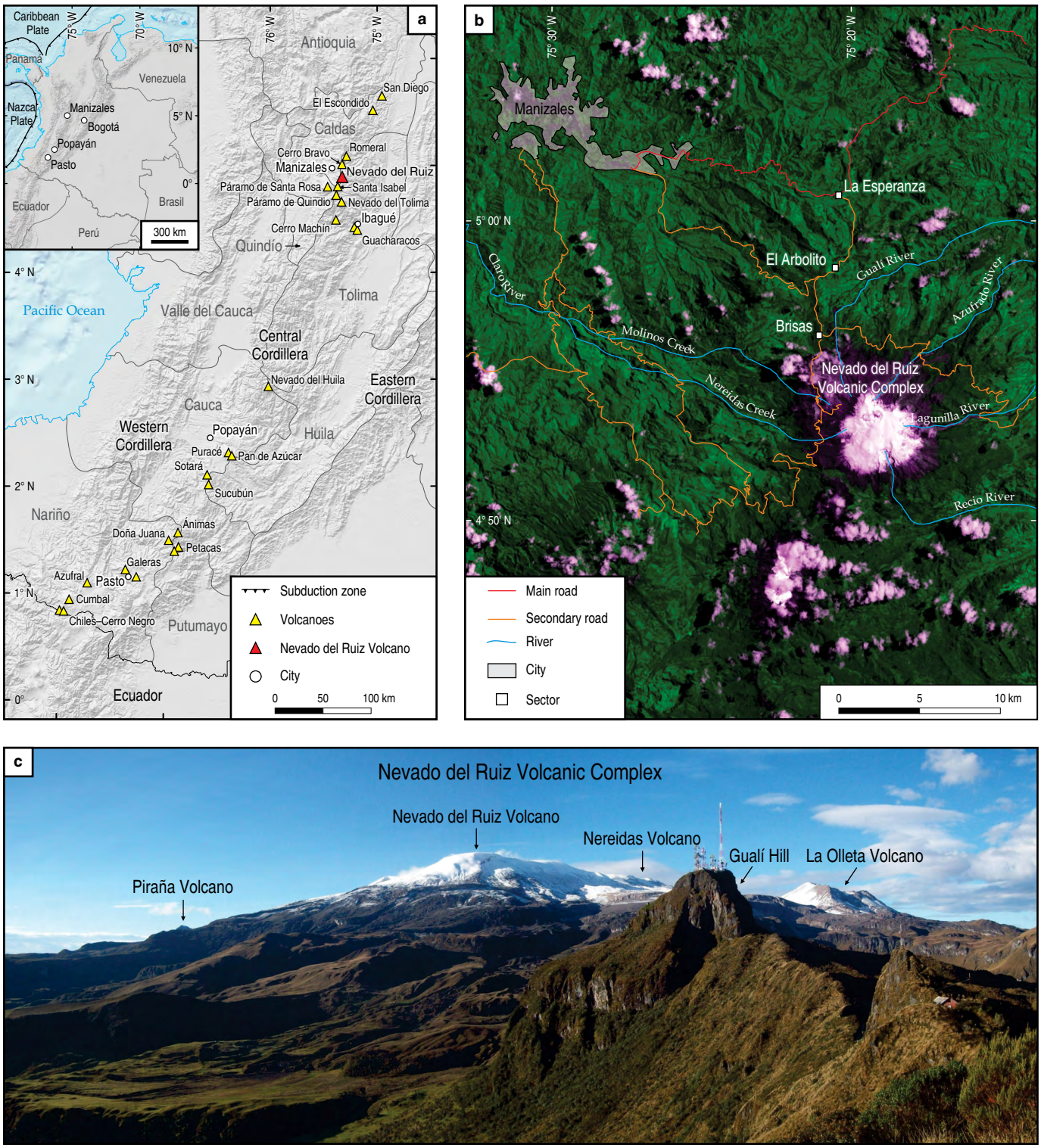

Figure 1. (a) Localization of the NRVC. **(b)** Main and secondary roads near to NRVC. **(c)** View of the NRVC from the NW.

synthetic aperture radar (UAVSAR) images, which have 30 m (Shuttle Radar Topography Mission [STRM] of the National Aeronautics and Space Administration [NASA]) and 12.5 m (Sensor ALOSPALSAR of the Japan Aerospace Exploration Agency [JAXA]) digital elevation model (DEM) resolutions. The morphological analysis also used aerial photographs at scales ranging from 1:23 000 to 1:50 000 from different years from the Instituto Geográfico Agustín Codazzi (IGAC).

Eruptive units were defined according to Fisher & Schmincke (1984), the volcanic deposits were classified based on Murcia et al. (2013), and the interpretation of the geology and stratigraphy of the mapped deposits was summarized by

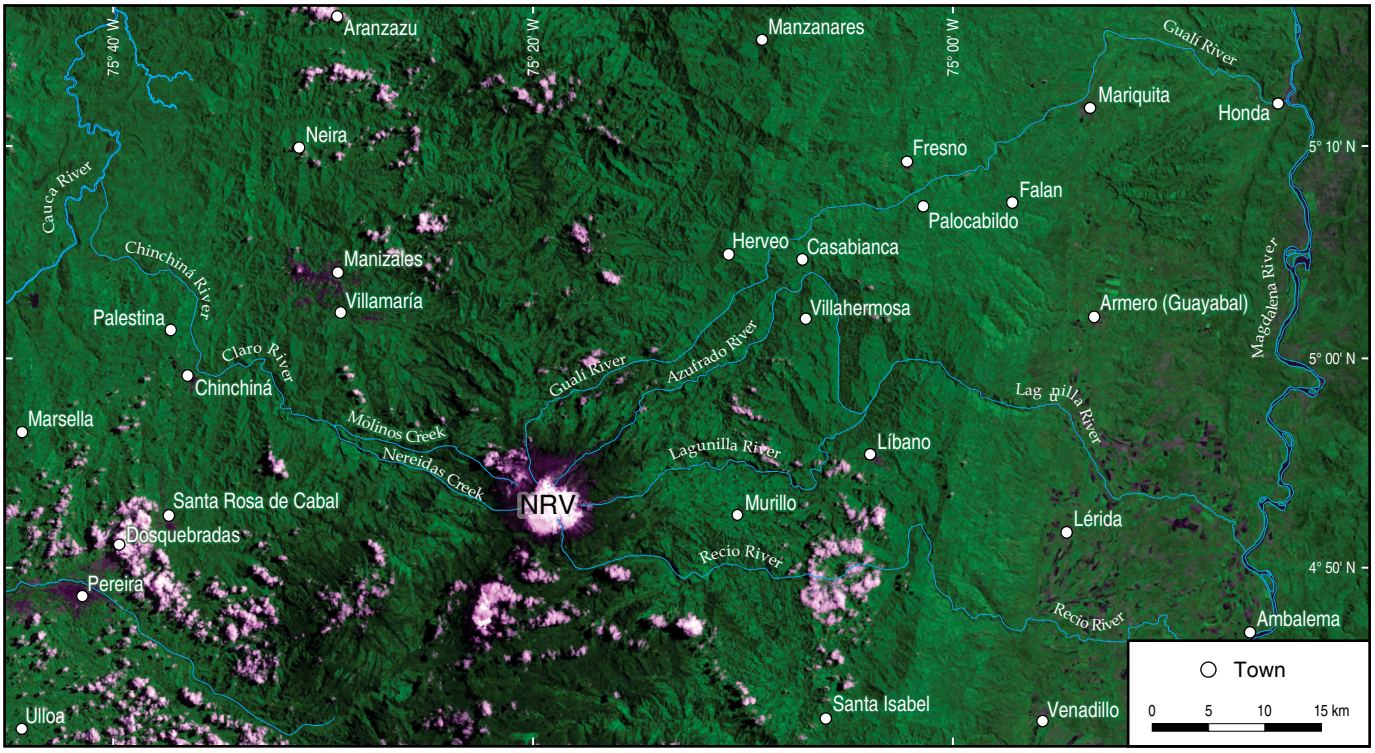

Figure 2. Main drainage system of the NRV.

partly adopting the method proposed by Lucchi (2013). This method meets the highest demands set by the International Association of Volcanology and Chemistry of the Earth's Interior (IVACEI) for geological research in volcanic areas. This method aims to describe the types of volcanic rocks and deposits, reconstruct their vertical succession and their changes over time, characterize units bordered by unconformities, define their genesis and sources, and establish correlations among various rock units considering the complex, diverse, and episodic characteristics of the dominant processes in volcanic areas. Currently, this method has been applied in Colombia by the Grupo de Geología de Volcanes of the SGC on the Doña Juana Volcanic Complex (Pardo et al., 2016, 2019) and on the Paramillo de Santa Rosa Volcanic Complex (Pulgarín–Alzate et al., 2020). These studies used concepts from the International stratigraphic guide (Salvador, 1994) and involved the integrated use of lithological units combined with chronostratigraphic units, which led to the definition of lithostratigraphic units, lithosomes, and unconformities (Martí et al., 2018). The basic stratigraphic unit corresponds to a rock body delimited at the base and top by designated, significant, and demonstrable unconformities or discontinuity surfaces. In this hierarchy, first–order unconformities occur at a regional scale and affect several volcanoes, second–order unconformities involve a large section of a volcano, and third–order unconformities affect a sector of a volcano. Local discontinuities controlled by transport–emplacement mechanisms (diastems) are useful for identifying transport/accumulation volcanic processes but not for stratigraphic correlations.

The volcanic deposits were grouped into major categories with temporal significance according to Fisher & Schmincke (1984); thus, the eruptive pulse (lasting from seconds to minutes), the eruptive phase (from minutes to days), and several eruptions (volcanic activity occurring over days, months, or years) in an eruptive unit are grouped into an eruptive epoch (which corresponds to a time period of tens, hundreds, or thousands of years), and several eruptive epochs form an eruptive period (which may last from thousands to millions of years).

The granulometry, components, petrography, and geochemistry of representative samples of the NRVC were analyzed using inductively coupled plasma mass spectrometry (ICP–MS) and X–ray fluorescence and the major, minor, and trace elements were measured. The analyses were performed in the laboratories of the SGC. To determine the ages of the different NRVC eruptive periods and of the most relevant events, (8) samples were dated using the $^{40}Ar/^{39}Ar$ method at the Argon Geochronology Laboratory of Oregon State University, USA (Table 1). To calibrate the temporality of the most recent eruptive episodes, (41) samples of organic material (carbons and paleosols) were dated (Tables 2, 3) using the ^{14}C method at the geochronology laboratory of the University of Zurich Switzerland, and other samples were dated at Beta Analytic Inc., Miami, USA. In addition, K–Ar and ^{14}C radiometric ages measured by Herd (1974), Lescinsky (1990), and Thouret et al. (1990) were referenced.

The integration of these tools and the new results from radiometric dating is one of the most significant contributions of the

Table 1. $^{40}Ar/^{39}Ar$ dating performed at the NRVC.

Plateau age	Sample	Latitude N	Longitude W	Eruptive unit	Type of rock	Material	Plateau						
							± 2σ (f)	^{39}Ar	K/Ca	± 2σ	MSWD	P	n	N
26.8 ± 5.7 ka	NRAC–004	4° 54' 39.25"	75° 19' 48.13"	SEPR lava flows	Andesitic Lava	Groundmass		Width						
95.4 ± 7.0 ka	NRGV–28–1	4° 56' 13.65"	75° 28' 52.81"	Río Claro eruptive unit	Ignimbrite	Plagioclase	Excellent PLAG PLAT age	1	0.089	0	1.72	0.01	29	29
	NRGV–28–1			Río Claro eruptive unit	Ignimbrite	Clinopyroxene	Discordant age spectra of an ultra–low–K CPX with K/Ca = 0.0069							27
1033.3 ± 3.4 ka	NRJR–19	5° 1' 16.61"	75° 11' 29.96"	Pre–Ruiz lava flows	Andesitic lava	Groundmass	Excess 40/36(atm) = 309.2 ± 0.539 %SD; excellent GM PLAT age	0.88	1.091	0.194	0.98	0.48	19	25
107.3 ± 6.2 ka	NRSN–025	4° 53' 0.80"	75° 21' 11.53"	La Olleta Volcano	Andesitic lava	Plagioclase	Subatmospheric 40/36(atm) = 281.7.0 ± 2.28 %SD; good PLAG PLAT age	0.92	0.099	0.001	1.38	0.09	29	31
101.5 ± 7.4 ka	NRSN–025			La Olleta Volcano	Andesitic lava	Plagioclase	Subatmospheric 40/36(atm) = 281.7.0 ± 2.28 %SD; good PLAG PLAT age	1	0.099	0.001	2.11	0	29	29
104.3 ± 4.8 ka	NRSN–025			La Olleta Volcano	Andesitic lava		Subatmospheric 40/36(atm) = 281.7.0 ± 2.28 %SD; good PLAG PLAT age	0.95	0.099	0.001	1.76	0	58	60
66.3 ± 5.6 ka	NRSN–101	4° 56' 10.69"	75° 20' 33.24"	SEPR lava flows	Andesitic lava	Plagioclase	Excellent PLAG PLAT age	1	0.101	0.001	1.49	0.05	28	28

present study because the use of stratigraphic unconformities and ages of the deposits enables a clear definition of the time markers that are critical for understanding the stratigraphic sequence and in its interpretation regarding the evolution of the NRVC.

3. Geological Setting

The NRVC is located in the northernmost section of the North Volcanic Zone of the Andean volcanic belt defined by Gansser (1973). Tectonically, this zone corresponds with the subduction of the Nazca Plate under the South American Plate, which occurs at a rate of 55 mm/year and an azimuth of 88° and at 53 mm/year and an azimuth of 86°, according to data from the Geodesia: Red de Estudios de Deformación (GeoRED) project of the SGC (Mora et al., 2016). This subduction creates a very narrow volcanic arc (Trenkamp et al., 2002) above the Benioff seismogenic area, which defines the area where the subducted oceanic plate dips at 45° (Bourdon et al., 2003). In Colombia, the thickness of the continental crust under the volcanic arc of the Central Cordillera ranges from 40 to 55 km (Meissner et al., 1980; Restrepo–Pace, 1992). The oblique collision between the Nazca and South American Plates favors a shortening and inversion of the NE–SW continental structures and generates a transpressive domain and new ENE–WSW shear structures due to the differential reactivation of fault systems parallel to the Andes and the reactivation of pre–existing NW–SE structures (Toro & Osorio, 2005).

The rocks of the basement in the area proximal to the NRVC are metamorphic rocks from the Cajamarca Complex, intrusive igneous bodies of the Manizales Stock and El Bosque Batholith, and volcaniclastic deposits of the Manizales and Casabianca Formations. The Cajamarca Complex (Feininger et al., 1972; González, 1989; Nelson, 1957) corresponds to metamorphic rocks, including graphitic schists, moscovitic, chloritic, and amphibole quartz phyllites, and quartzites located between the San Jerónimo (to the W) and Otú–Pericos

Table 2. Eruptive units of the last 13 ka in the NRV.

Eruptive Unit	Eruptive dynamic	Ages ^{14}C (y BP)
13 400 BP	Phreatomagmatic eruptions. Several eruptive pulses. PDC were generated.	Charcoal ages: 13 400 ± 60, 13 483 ± 43, and 13 520 ± 60.
10 400 BP	Phreatomagmatic eruptions. Several eruptive pulses. PDC were generated.	Charcoal ages: 10 490 ± 50 and 10 439 ± 34.
8500 BP	Phreatomagmatic eruption. PDC originate by column collapse. Pyroclastic falls.	Paleosol ages: 8379 ± 34, 8683 ± 33, 8520 ± 40, and 8550 ± 40. Charcoal ages: 8170 ± 50.
6000 BP	Phreatomagmatic eruptions. Several eruptive pulses. PDC were generated.	Charcoal ages: 5964 ± 29, 6050 ± 40, 6174 ± 28, and 6550 ± 40.
3300 BP	Phreatomagmatic eruption. Subplinian style. Pyroclastic falls. PDC originate by column collapse.	Charcoal ages: 3312 ± 26, 3359 ± 27, 3360 ± 30, and 3570 ± 30. Paleosol ages: 2910 ± 30 and 3030 ± 30.
2100 BP	Phreatomagmatic eruption. Subplinian style. Pyroclastic falls. PDC originate by column collapse.	Charcoal ages: 2020 ± 30 and 2110 ± 30, 2170 ± 30, 2180 ± 30, and 2220 ± 30.
1500 BP	Phreatomagmatic eruption. Pyroclastic falls. PDC dilute, originate by column collapse.	Charcoal age: 1520 ± 30.
1200 BP	Several eruptive pulses. Explosion and collapse volcanic domes preexisting. Eruptive column collapse. Pyroclastic falls and PDC.	Paleosol age: 1140 ± 30 (SGC) and 1275 ± 50 (Thouret et al., 1985).
1000 BP	Phreatomagmatic eruptions. Several eruptive pulses.	Charcoal age: 920 ± 30, 993 ± 24, 980 ± 30, 1000 ± 30, and 980 ± 30.
800 BP	Phreatomagmatic eruption. Pyroclastic falls. PDC originate by column collapse.	Paleosol age: 780 ± 90 and 840 ± 60 (Thouret et al., 1985).
600 BP	Phreatomagmatic eruptions. Several eruptive pulses. PDC were generated.	Charcoal ages: 610 ± 24, 540 ± 30, and 622 ± 33.
1595 AD	Phreatomagmatic eruption. Two (2) pulses. Subplinian style. Pyroclastic falls. PDC originate by column collapse. Lahars by Chinchiná, Claro, Gualí, Azufrado, and Lagunilla Rivers. Armero sector was affected.	Charcoal ages: 470 ± 30 and 400 ± 30.
1800 AD	Phreatomagmatic eruptions? Several pulses? Pyroclastic falls. PDC originate by column collapse. In 1845 AD, noneruptive phenomena generated lahars by Gualí, Azufrado, and Lagunilla Rivers. Armero sector was affected.	Charcoal ages: 100 ± 25, 110 ± 30, 114 ± 24, and 126 ± 25.
1985 AD	Phreatomagmatic eruption. Subplinian style. Pyroclastic falls. PDC originate by column collapse. Lahars by Chinchiná, Claro, Gualí, Azufrado, and Lagunilla Rivers. Armero and Chinchiná sectors were affected.	

(to the E) Faults; these rocks include the Tahamí Terrane, which experienced Triassic age metamorphism according to the Geological Map of Colombia 2015 version by Gómez et al., (2015). The Manizales Stock, which is composed of quartz dioritic–tonalitic composition (Aguirre & López, 2003), has ages ranging from 56 to 57 Ma (Brook, 1984) and 43.9 Ma (Villagómez, 2010). El Bosque Batholith outcrops in the E sector of the NRVC and has a predominantly granodioritic–tonalitic composition and an age of 49.1 Ma (Vesga & Barrero, 1978). The Manizales Formation of Miocene – Pliocene age (Flórez, 1986; Herrera & López, 2003; Naranjo & Ríos, 1989) and the Casabianca Formation (Borrero & Naranjo, 1990) of Pliocene – Pleistocene age correspond to primary, secondary, and epiclastic volcanogenic deposits, the volcanic sources of which are not evident in the geological record.

According to Bohórquez et al. (2005), the NRV area, which is integrated into the area of volcanism in the Cerro Bravo–Cerro Machín zone, is emplaced in a microblock bordered by the Río Arma Fault to the N, the Ibagué Fault to the S, the San Jerónimo Fault to the W, and the Mulatos Fault to the E. In the proximal–central area of the NRVC, four structure systems stand out: those that have right–lateral transcurrent movement in the NE–SW direction, which correspond to the Palestina Fault System (N10°–30°E) and affect the central area of the NRV edifice, and the Santa Rosa Fault (N60°–70°E), which controls most of the Gualí River Basin. These structures also show minor synthetic lineaments concentrated on the NW (Brisas sector and N of La Olleta) and NE (Azufrado River headwaters) flanks of the NRV. Structures with NW–SE and ENE–WSW trending transcurrent and distensive characteristics correspond to the Villamaría–Ter-

Table 3. List of ^{14}C dating.

Sample	Age y BP	Sample type	Location*		Eruptive unit	Laboratory
			Latitude N	Longitude W		
VNRLM–47–3	100 ± 25	Charcoal	4° 56' 17.517"	75° 21' 53.542"	1840 AD	University of Zurich
VNRLM–31–G–3	110 ± 30	Charcoal	4° 53' 0.330"	75° 22' 30.169"	1840 AD	Beta Analytic Inc.
VNRLM–28–A1–3	114 ± 24	Charcoal	4° 53' 30.57"	75° 22' 53.490"	1840 AD	University of Zurich
VNRLM–56–B–3	126 ± 25	Charcoal	4° 58' 53.90"	75° 20' 20.83"	1840 AD	University of Zurich
NRGV–86–F–3	380 ± 30	Paleosol	5° 13' 26.389"	74° 47' 44.694"	1595 AD	Beta Analytic Inc.
NRIZ–83–C–3	400 ± 30	Paleosol	5° 12' 45.071"	74° 53' 29.738"	1595 AD	Beta Analytic Inc.
NRIZ–82–D–3	470 ± 30	Paleosol	5° 12' 35.874"	74° 53' 30.167"	1595 AD	Beta Analytic Inc.
VNRLM–99–3	610 ± 24	Charcoal	4° 53' 1.620"	75° 22' 59.324"	600 BP	University of Zurich
NRLN–1–J–3	540 ± 30	Charcoal	4° 56' 28.705"	75° 15' 27.500"	600 BP	Beta Analytic Inc.
VNRLM–34–C–3	622 ± 33	Charcoal	4° 56' 3.984"	75° 28' 5.250"	600 BP	Beta Analytic Inc.
NRSN–97–F–3	920 ± 30	Charcoal	4° 50' 33.976"	75° 16' 30.622"	1000 BP	Beta Analytic Inc.
VNRLM–100–B–3	993 ± 24	Charcoal	4° 53' 5.310"	75° 23' 4.730"	1000 BP	University of Zurich
NRLM–123–E–3	980 ± 30	Charcoal	4° 53' 3.355"	75° 23' 1.996"	1000 BP	Beta Analytic Inc.
NRLM–123–G–3	1000 ± 30	Charcoal	4° 53' 3.355"	75° 23' 1.996"	1000 BP	Beta Analytic Inc.
NRHM–50–B–3	1140 ± 30	Charcoal	4° 55' 32.374"	75° 17' 43.159"	1000 BP	Beta Analytic Inc.
NRAC–52–D–1	1520 ± 30	Charcoal	4° 56' 0.243"	75° 19' 6.642"	1500 BP	Beta Analytic Inc.
NRJR–16–E–3	2180 ± 30	Charcoal	4° 57' 37.116"	75° 16' 42.748"	2100 BP	Beta Analytic Inc.
NRJR–16–D–3	2020 ± 30	Charcoal	4° 57' 37.116"	75° 16' 42.748"	2100 BP	Beta Analytic Inc.
NRAC–52–D–3	2110 ± 30	Charcoal	4° 56' 0.243"	75° 19' 6.642"	2100 BP	Beta Analytic Inc.
NRSN–66–F–3	2170 ±30	Charcoal	4° 54' 19.012"	75° 14' 59.087"	2100 BP	Beta Analytic Inc.
VNRLM–23–C–3	2220 ± 30	Charcoal	4° 53' 57.167"	75° 14' 59.946"	2100 BP	Beta Analytic Inc.
VNRLM–22–C–3	2910 ± 30	Paleosol	4° 54' 15.829"	75° 14' 58.380"	3300 BP	Beta Analytic Inc.
NRHM–50–A1–3	3030 ± 30	Paleosol	4° 55' 32.374"	75° 17' 43.159"	3300 BP	Beta Analytic Inc.
VNRLM–31–D–3	3312 ± 26	Charcoal	4° 53' 0.330"	75° 22' 30.169"	3300 BP	University of Zurich
ANRJC–12–B–3	3359 ± 27	Charcoal	4° 54' 22.469"	75° 22' 32.265"	3300 BP	University of Zurich
NRSN–97–C–3	3360 ± 30	Charcoal	4° 50' 33.976"	75° 16' 30.622"	3300 BP	Beta Analytic Inc.
NRJR–16–B–3	3570 ± 30	Charcoal	4° 57' 37.116"	75° 16' 42.748"	3300 BP	Beta Analytic Inc.
VNRLM–1–C2–3	5964 ± 29	Charcoal	4° 53' 33.276"	75° 24' 4.316"	6000 BP	University of Zurich
NRJR–32–6–3	6050 ± 40	Charcoal	4° 55' 32.887"	75° 22' 49.332"	6000 BP	Beta Analytic Inc.
VNRLM–93–C	6174 ± 28	Charcoal	4° 55' 53.950"	75° 19' 28.370"	6000 BP	University of Zurich
NRLN–2–G–3	6550 ± 40	Charcoal	4° 56' 24.839"	75° 15' 36.558"	6000 BP	Beta Analytic Inc.
NRIZ–27–3	8170 ± 50	Charcoal	4° 56' 42.990"	75° 31' 20.589"	8100 BP	Beta Analytic Inc.
VNRLM–96–A–3	8379 ± 34	Paleosol	4° 50' 41.622"	75° 23' 32.749"	8100 BP	University of Zurich
NRLN–2–J–3	8520 ± 40	Paleosol	4° 56' 24.839"	75° 15' 36.558"	8100 BP	Beta Analytic Inc.
NRSN–77–D–3	8550 ± 40	Paleosol	4° 54' 29.854"	75° 13' 3.970"	8100 BP	Beta Analytic Inc.
VNRLM–95–A–3	8683 ± 33	Paleosol	4° 51' 30.743"	75° 21' 50.577"	8100 BP	University of Zurich
NRLN–4–C–3	10 490 ± 50	Charcoal	4° 57' 25.744"	75° 11' 48.912"	10 400 BP	Beta Analytic Inc.
VNRLM–102	10 439 ± 34	Charcoal	4° 53' 42.190"	75° 24' 18.090"	10 400 BP	University of Zurich
NRGV–33–3	13 400 ± 60	Charcoal	4° 54' 26.006"	75° 25' 49.912"	13 400 BP	Beta Analytic Inc.
VNRLM–27–A–3	13 483 ± 43	Charcoal	4° 54' 5.886"	75° 13' 3.648"	13 400 BP	U. de Zurich
NRLN–5–D–3	13 520 ± 60	Charcoal	4° 57' 19.411"	75° 11' 47.324"	13 400 BP	Beta Analytic Inc.

*WGS84 reference system.

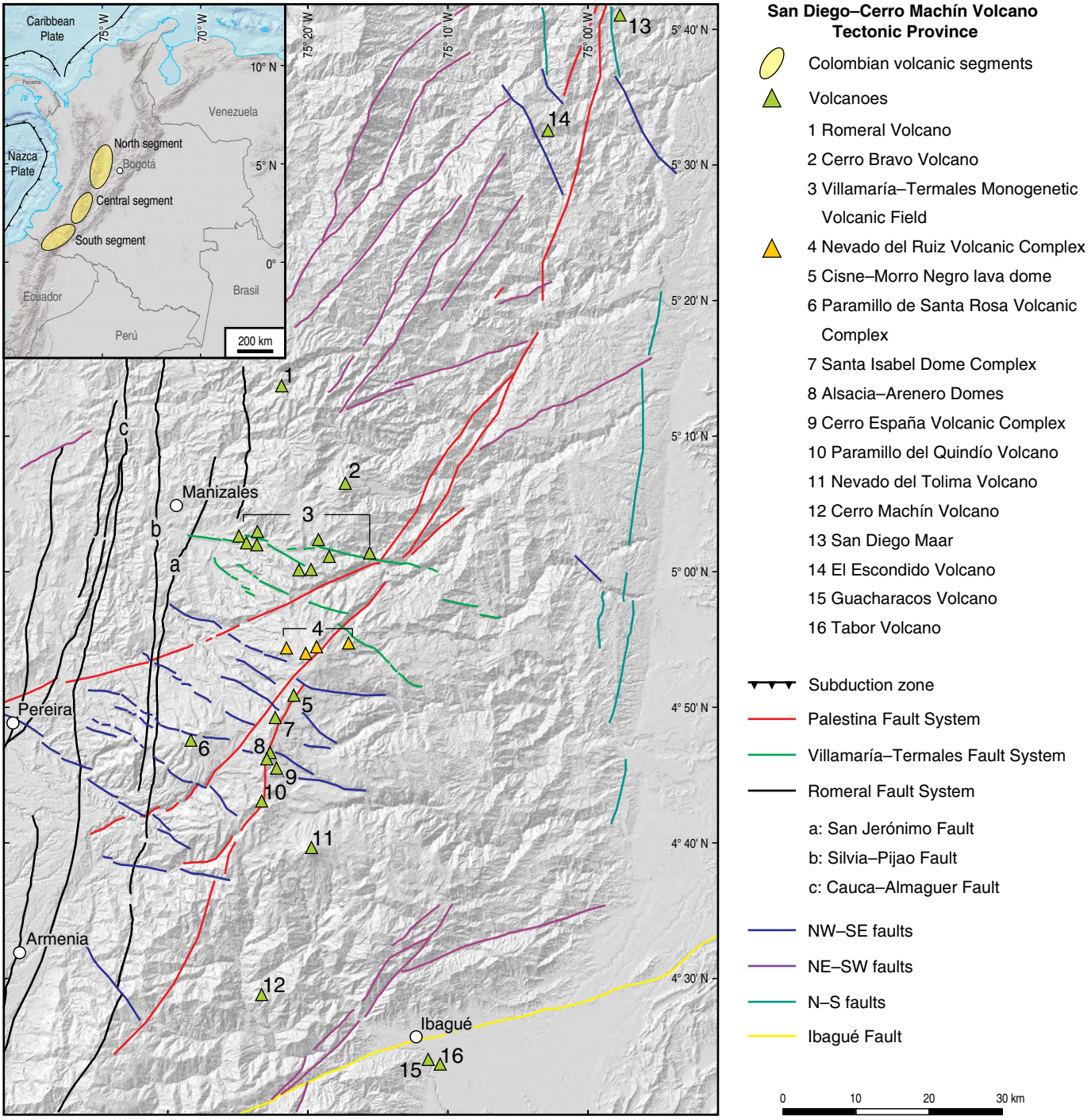

Figure 3. Localization of the San Diego–Cerro Machín Volcano Tectonic Province (SCVTP), north segment.

males Fault System (VTFS), Nereidas Fault, and Río Claro Fault. Structures with N–S and NNE–SSW trends affect the W flank of the NRVC between the NRV and the San Jerónimo Fault.

The NRVC is part of a larger volcanic area that includes several complexes and volcanic centers that, when grouped, form a volcanic province (according to Fisher & Schmincke, 1984 and Pujadas et al., 1999). The NRVC has been proposed to be included in this volcanic province, named the San Diego–Cerro Machín Volcano Tectonic Province (SCVTP).

The NRVC is located at the center of the SCVTP (Martínez et al., 2014) and is part of the northern segment of active volcanoes in Colombia (Figure 1a). The SCVTP is composed of volcanic complexes, a polygenetic volcanic chain, and monogenetic volcanic fields (Figure 3). The San Diego Maar, El Escondido Volcano, Romeral Volcano, Cerro Bravo Volcano, Villamaría–Termales Monogenetic Volcanic Field, NRVC, Cisne–Morro Negro lava dome, Santa Isabel Dome Complex, Paramillo de Santa Rosa Volcanic Complex, Cerro España Vol-

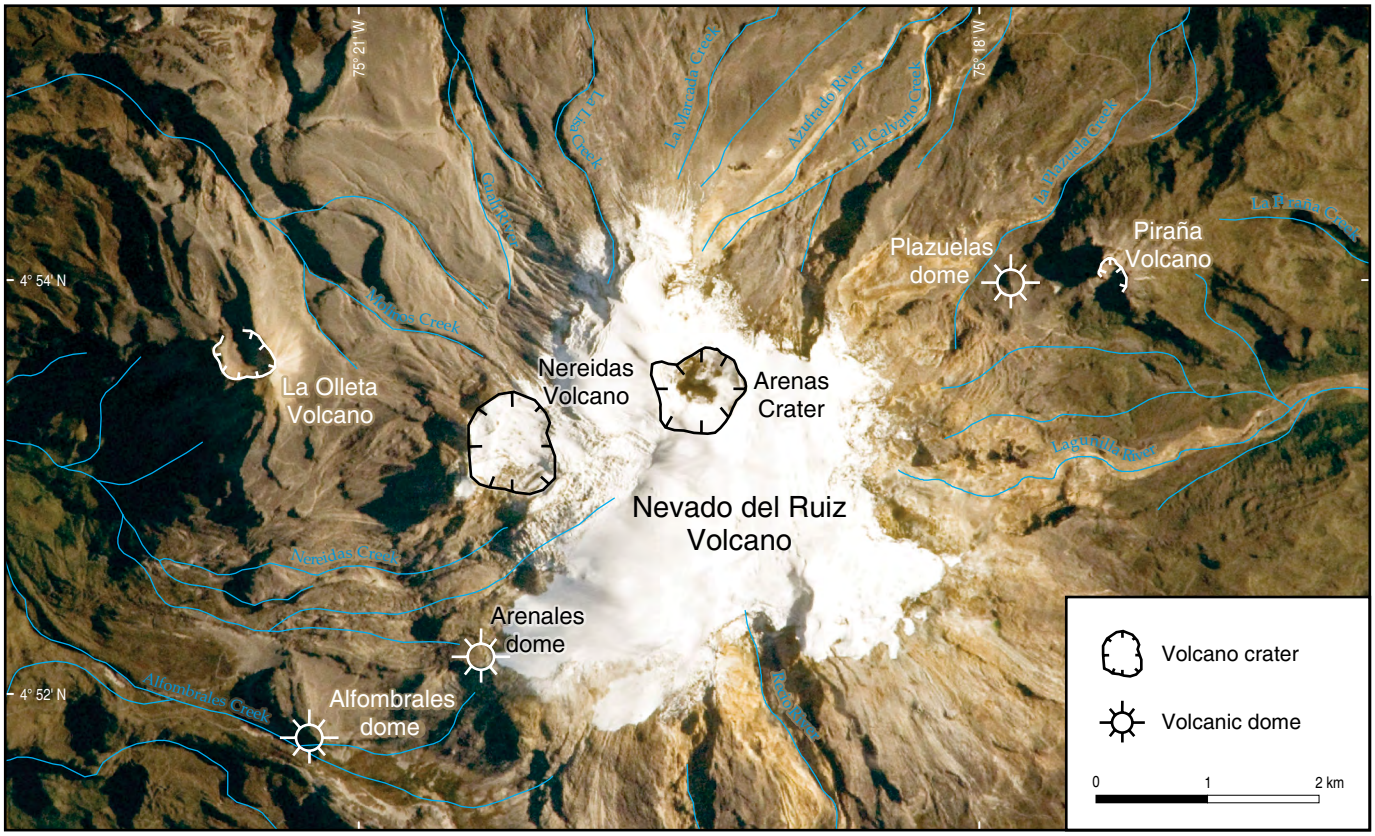

Figure 4. View of the NRVC from space in 2012 (Image Science and Analysis Laboratory, NASA – Johnson Space Center: The Gateway to Astronaut Photography of Earth).

canic Complex, Paramillo del Quindío Volcano, Nevado del Tolima Volcano, Cerro Machín Volcano, and Guacharacos and Tabor volcanic centers are present from north to south.

4. Nevado del Ruiz Volcanic Complex

An assemblage of deposits and volcanic structures that are spatially, temporally, and genetically associated with the development of the NRV is included in the NRVC. According to de Silva & Francis (1991), a volcanic complex is a set of spatially extensive major and minor eruptive centers that are spatially, temporally, and genetically related, for example, the Tongariro Volcanic Complex (Hobden et al., 1996).

The NRVC (Figures 1c, 4) is currently formed by remnants of the "Ancestral Ruiz" and "Older Ruiz" edifices, the NRV and its Arenas Crater (Figures 4, 5a), the surrounding volcanoes, such as La Olleta to the W (Figure 5b), Piraña to the E (Figure 5c), and Nereidas to the SW (Figure 5d), the Arenales and Alfombrales domes SW of the NRV (Figure 6a, 6b), and the Plazuelas dome (Figure 6c) NE of the NRV.

The deposits and geological structures defined in the geological map of the NRVC (Figure 7a, 7b) include in the proximal area of the NRV, the volcanoes and surrounding domes, and the primary and secondary volcaniclastic deposits found in the valleys and drainage divides of La Lisa, La Marcada, Aguas Calientes, El Calvario, and La Plazuela headwaters, the Gualí, Azufrado, Lagunilla, and Recio Rivers, which flow eastward, and the Molinos, Nereidas, and Alfombrales headwaters, which flow westward. The distal zone of the NRVC, in the W sector, includes the Pleistocene – Holocene volcanic deposits outcropping in the lower Claro, Chinchiná, and Cauca River Basins. The E sector of the NRVC includes the deposits outcropping in the distal areas of the Gualí, Azufrado, Lagunilla, and Recio Rivers mouths along the Magdalena River. The volcanic deposits of the Mariquita Fan, the Lérida Fan, and the Antiguo Armero area are also included.

Based on geomorphological and geological characterizations and stratigraphic calibration using radiometric dating conducted in the present study, and complemented by data reported by other authors, a series of volcanic structures with ages ranging from ca. 1.8 Ma to the present are grouped in the NRVC; such volcanic structures are formed by lava flows, pyroclastic density currents (PDC) and pyroclastic falls deposits, secondary volcaniclastic deposits (debris avalanches and lahars), and glacial and fluvial deposits. Based on the data collected, the geological evolution of the NRVC is divided into four eruptive periods: The Pre–Ruiz eruptive period, First eruptive period Ruiz, Intermediate eruptive period Ruiz, and Second eruptive period Ruiz.

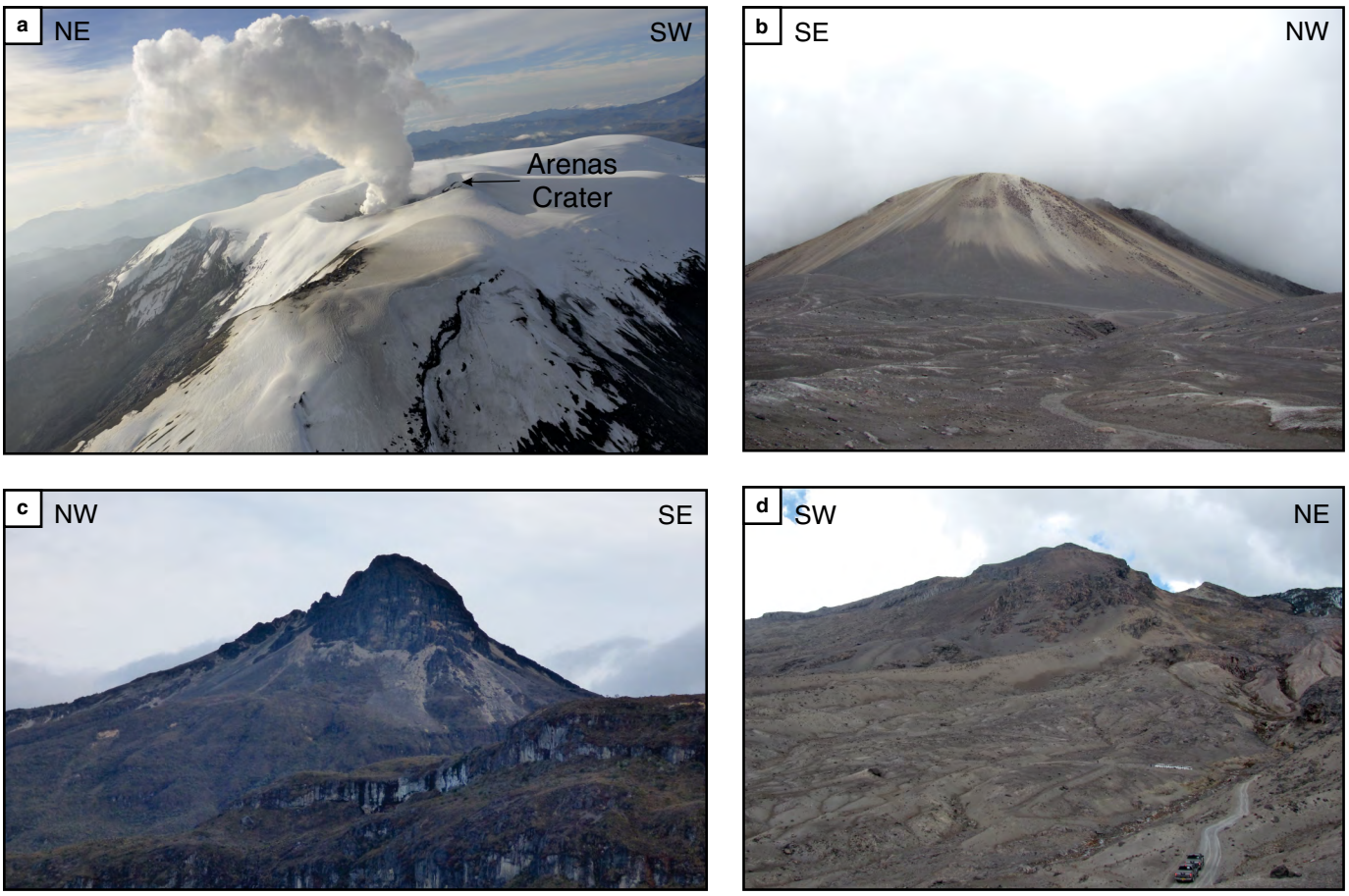

Figure 5. Main volcanic edifices of the NRVC. **(a)** NRV. **(b)** La Olleta Volcano. **(c)** Piraña Volcano. **(d)** Nereidas Volcano.

4.1. Pre–Ruiz Eruptive Period

This eruptive period was characterized by effusive volcanism and its products are very thick and homogeneous sequences of andesitic lava flows. Their radial distribution suggests that the emission center (or perhaps several centers) of the so–called "Ancestral Ruiz" volcano was located N of the current NRV in the upper Gualí River Basin, with remnants that include the Gualí and Recreo Hills (Figure 8a).

The lava flows PRE–LD form elongated and very eroded hills (Figure 8b) that reach altitudes of up to 200 m and a maximum length of up to 30 km, thereby forming the longest, largest, and thickest lobes of the NRVC. These flows are homogeneous and consist of massive layers with individual thicknesses ranging from 10 to 30 m with associated autobreccias and cooling structures in the form of very dense horizontal and subhorizontal joints with columnar jointed texture (Figure 8c). Petrographically, these deposits correspond to porphyritic hypocrystalline andesites, the matrices of which may range from microcrystalline to cryptocrystalline, with microlithic or trachytic variations and variable glass contents. Compositionally, they show a preferential mineral association (Figure 8d, 8e) formed by plagioclase, orthopyroxene, clinopyroxene, opaque minerals ± amphibole ± biotite. The plateau age was assessed to be 1.033 Ma using the $^{40}Ar/^{39}Ar$ dating method on the matrix of andesitic remnants of lava flow deposits with columnar jointed texture (Figure 8c) near the municipality of Casabianca (Carros de Piedra sector).

Lava flows are defined between two main unconformities (Figure 9), one of which is a regional first–order unconformity termed U_0, represented by the nonconformity that separates the metamorphic (Cajamarca Complex [Triassic]) rocks from the plutonic (Manizales Stock and Bosque Batholith [Paleocene–Eocene]) rocks and the volcaniclastic deposits (Manizales and Casabianca Formations [Miocene – Pleistocene]) of the lava flows from the "Ancestral Ruiz" volcanic edifice. This unconformity marks the start of the NRVC volcanism, is an R_1 second–order unconformity, and marks a stratigraphic hiatus between the end of the Pre–Ruiz volcanism and the start of the "Older Ruiz" volcano construction. The ages assigned to this eruptive period range from ca. 1.8 to ca. 0.97 Ma, according to dating by Thouret et al. (1990). The Pre–Ruiz eruptive period is equivalent to the Pre–Ruiz lavas period established by Schaefer (1995) and to the Ruiz Ancestral eruptive period termed by Thouret et al. (1990), and has three eruptive stages: the "Gualí" (1.8 ± 0.1 Ma), "Tesorito" (1.25 ± 0.1 – 1.2 ± 0.2 Ma), and "El Líbano" (1.05 ± 0.08 Ma –

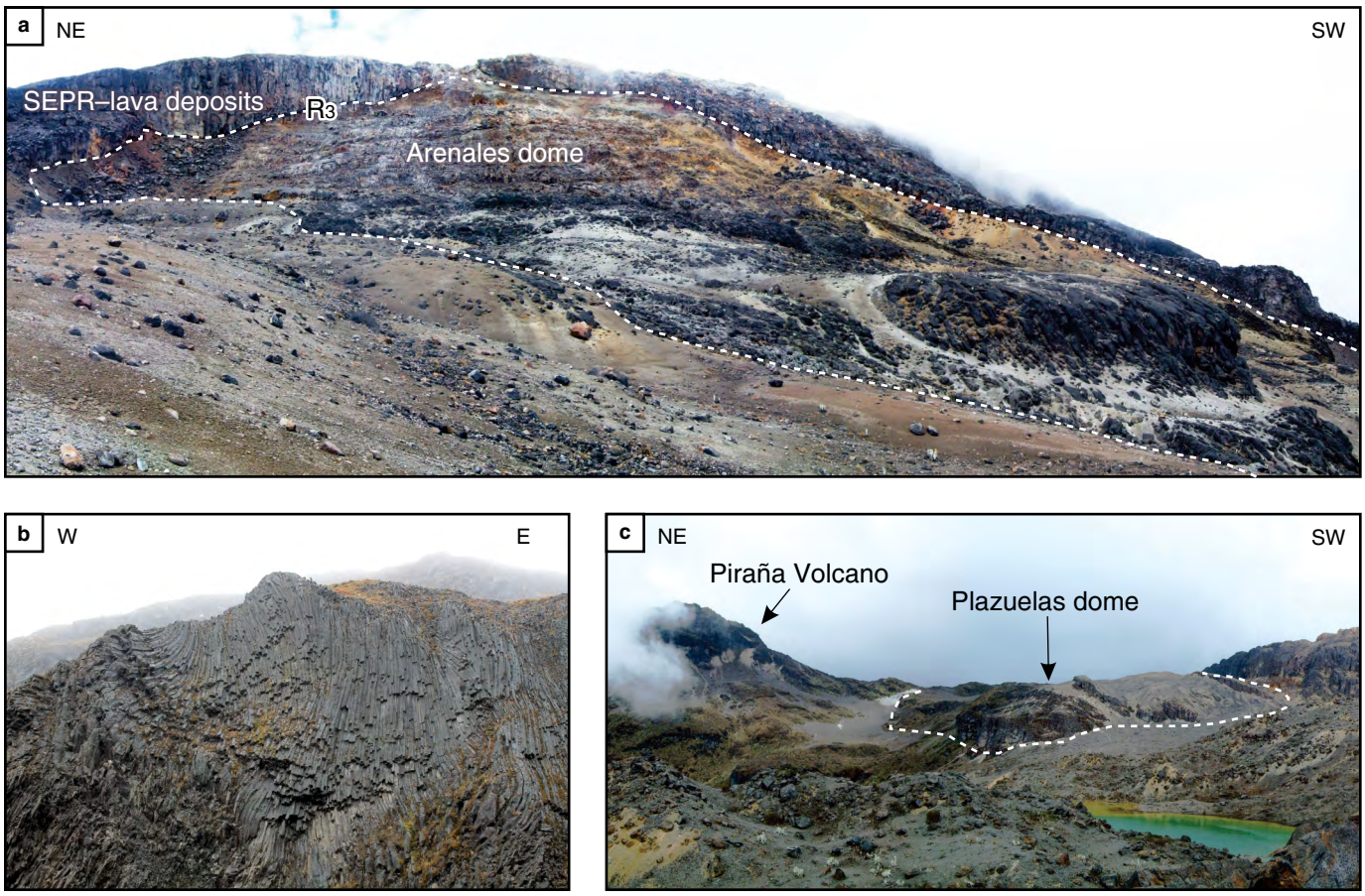

Figure 6. Main volcanic domes of the NRVC. **(a)** Arenales dome. Note the R_3 second–order unconformity. **(b)** Alfombrales dome. **(c)** Plazuelas dome.

0.97 ± 0.05 Ma), and also includes lava remnants (for example, the Gualí and El Arbolito Hills) and several altered domes. The authors describe these structures as products of the destructive phase of El Arbolito during the Ancestral Ruiz period (0.97 ± 0.05 Ma to 0.76 ± 0.05 Ma), which they propose to be a period of intracaldera resurgence. Therefore, El Arbolito Hill would be the edge of the collapse structure. However, in the present study, the formation of a caldera is unclear given the absence of associated ignimbrites and the remnants of the hills are argued to represent (Figure 8a) parts of the "Ancestral Ruiz" composite volcano.

The Pre–Ruiz effusive volcanism is possibly related to ancient fissures in the Palestina Fault System, and was synchronous with the effusive and explosive activity of the volcano Pre–Paramillo de Santa Rosa (ca. 2.5 to 0.8 Ma) of the Paramillo de Santa Rosa Volcanic Complex (Pulgarín–Alzate et al., 2020), and the emplacement of volcanic domes such as the Sancancio, Tesorito, Gallinazo, Amazonas, La Negra, and Sabinas (Aristizabal & Echeverry, 2001; Ayala, 2009; Borrero et al., 2009; Martínez et al., 2014; Murcia et al., 2017; Thouret et al., 1990; Toro et al., 2010; Vargas & Mann, 2013), which are aligned in the NW–SE direction along the Villamaría–Termales Fault System. The predominantly effusive volcanic activity preceded the Cerro Bravo, Paramillo del Quindío, and Nevado del Tolima volcanic eruptions, as shown by their K–Ar ages of 1.4 ± 0.25 Ma, 1.3 ± 0.15 Ma, and 1.29 ± 0.10 Ma, respectively, assessed by Thouret et al. (1990).

4.2. First Eruptive Period Ruiz

The First eruptive period Ruiz (FEPR) is divided into a first epoch of construction and a second epoch of destruction of the "Older Ruiz" volcanic edifice. The construction epoch is represented by lava flows (FEPR–LD) that cover an area of approximately 120 km^2 and are radially distributed, although they are more restricted than the lava flows of the Pre–Ruiz eruptive period. The thicknesses of the individual layers of the lava flows range from 5 to 60 m (25 m mean) and reach up to 9 km from the possible emission center. Petrographically, these lavas were classified as andesites, in which clinopyroxenes prevail over orthopyroxenes with variable quantities of amphibole and biotite. Based on the possible point of convergence in the reconstructions and the directions of the lava flows and volcaniclastic deposits of the FEPR, the possible emission center of this edifice should be located in a sector near the headwater of

Figure 7. (a) Geological Map of the NRVC. **(b)** Units: (PRE–LD) Pre–Ruiz eruptive period lava flows; (FEPR–LD) First eruptive period lava flows; (SI–DA) Santa Inés debris avalanche; (LI–DA) Líbano debris avalanche; (CH–VD) Chinchiná volcaniclastic deposits; (RC–EU) Río Claro eruptive unit; (LE–VD) Lérida volcaniclastic deposits; (OV) La Olleta Volcano; (PIV) Piraña Volcano; (NV) Nereidas Volcano; (PLD) Plazuelas dome; (AL–EU) Alfombrales eruptive unit; (ARL–EU) Arenales eruptive unit; (EFL) La Esperanza fissural lava; (VT–DA) Villamaría–Termales debris avalanche; (PL–DA) Playa Larga debris avalanche; (SEPR–LD) Second eruptive period Ruiz–lava flows; (NU) Nereidas Unit; (GF) glacier fluvial deposits; (RC–DA) Río Claro debris avalanche; (ARE–U) Arenas unit; (RM–LD) Río Molinos lahar deposit; (RE–EU) Recio eruptive unit; (LT–EU) Las Tumbas eruptive unit; (AC–VD) Arbolito Curubital volcanic domes; , this unit groups La Esperanza fissural lava deposits, La Laguna coulée dome, Santa Ana coulée dome, El Plato dome, and San Luis coulée dome (LD) lahar deposits; (M) moraines deposits; (QN–LD) Quebrada Nereidas lahar deposits; (LV–EU) La Vega eruptive unit; (PL–EU) Playa Larga eruptive unit; (MA–VD) Mariquita volcaniclastic deposits; (RA–DA) Río Azufrado debris avalanche; (MR–PD) Molinos River pyroclastic deposits; 13 400, 10 400, 8500, 6000, 3300, 2100, 1500, 1200, 800, and 600 BP eruptive units; (LA–LD) Lagunilla lahar deposit; 1595, 1800, and 1985 AD eruptive units; (CB**) Cerro Bravo Volcano fall pyroclastic deposits; (Qal– Qc) recent alluvial and colluvial deposits; (Uo) first–order unconformity; (R1, R2, R3) second order unconformities; (R3a, R3b, R3c) third order unconformities; (*) not mapped units.

the Recio River Basin, on the S and SE flanks of the current NRV edifice.

The basement of these deposits is defined by a second–order unconformity termed R_1 (Figure 9) that is evidenced by a subaerial erosion surface that marks a clear geomorphological contrast between the PRE–LD and FEPR lava flows. Thouret et al. (1990) reported a K–Ar age of 0.2 ± 0.05 Ma from an andesite. The age of onset of this eruptive period remains unknown and should range between 0.97 and 0.2–0.165 Ma. The R_1 would correspond to a stratigraphic hiatus that may have lasted between 0.6 and 0.2 Ma.

The volcanism of the first epoch of the FEPR may be correlated with the constructive epoch of the Paramillo de Santa Rosa Volcano (0.568 to 0.26 Ma) of the Paramillo de Santa Rosa Volcanic Complex (Pulgarín–Alzate et al., 2020), and with the effusive volcanic activity preceding the Santa Isabel Dome Complex and the Paramillo del Quindío and Nevado del Tolima Volcanoes, according to the ages (0.76 Ma, 0.68 Ma, 0.37 Ma, and 0.33 Ma) assessed by Thouret et al. (1990). The first stage of La Olleta Volcano formation began at the end of this constructive epoch; a plateau age assessed by $^{40}Ar/^{39}Ar$ dating of plagioclase in the andesitic lava was measured to be 107.3 ± 6.2 Ma.

El Líbano debris avalanche deposit of noneruptive origin occurs in the E flank of the NRVC. This deposit resulted from the flank collapse of the "Older Ruiz" volcano, covers an area of 86 km^2, and has a geomorphology of large mounds, atop which the towns of Murillo and El Líbano are currently located. This avalanche traveled approximately 28 km from its source and had an estimated volume of 6 km^3. Thouret et al. (1990) dated an andesite block from this deposit to be 0.165 Ma. In this study, the deposit is interpreted to represent a debris avalanche with an age younger than 0.165 Ma.

The secondary and epiclastic volcaniclastic deposits of Chinchiná outcrop towards the Chinchiná River Basin. The facies associations of these deposits suggest that lahar (debris flow facies) and epiclastic (torrential flow facies) deposits were accumulated during this eruptive period.

The second epoch of this eruptive period was explosive and is characterized by the formation of thick deposits of PDC with a facies association corresponding to an ignimbrite (Figure 10a–d), ranging from welded to unwelded. Based on geological mapping and component analysis, the Río Claro ignimbrite deposits (Grand & Handszer, 1989), the deposits of PDC in the lower Chinchiná River Basin that outcrop in the distal zone W of the NRCV and in the upper section of the Recio River Basin in the SE flank are integrated in the Río Claro eruptive unit (RC–EU). This unit was calculated to be approximately 5 km^3 in volume, with a mean thickness of 200 m and an area of 25 km^2. Similarly, other deposits from pyroclastic density currents and ignimbrite fallout deposits, the distribution of which reaches more than 60 km W and more than 40 km E of the current NRV, were included within the second epoch of the FEPR. The emitted volume indicates the formation of a caldera (Figure 11) resulting from the destruction of the "Older Ruiz" volcano. The remobilization of these pyroclastic deposits and the syneruptive generation of lahars (hyperconcentrated flows) produced the volcaniclastic deposits that formed the Lérida Fan. The facies associations found in the Lérida Fan (Figure 12) suggest the presence of three segments. The basal segment is interpreted to be deposits produced by the filling of river channels located in the apex of an old alluvial fan, resulting from the accumulation of material associated with fluvial–torrential flows that filled and overflowed channels. The intermediate segment's deposits correspond to diluted lahars (hyperconcentrated flow facies) associated with the remobilization of pyroclastic deposits of the RC–EU. Last, the deposits of the upper segment were interpreted as both concentrated (debris flows) and diluted (hyperconcentrated flows) lahar deposits, which progressively transformed into fluvial and epiclastic deposits (braided streams and paleochannel filling).

Thouret et al. (1990) determined K–Ar ages of plagioclase in an andesite from the Río Claro ignimbrite of 0.2 ± 0.07 Ma and 0.2 ± 0.05 Ma from whole rock samples. These ages indicate crystallization of lava flows from the construction epoch of the "Older Ruiz", which were subsequently fragmented and incorporated into PDC. In this study, a new $^{40}Ar/^{39}Ar$ plateau age

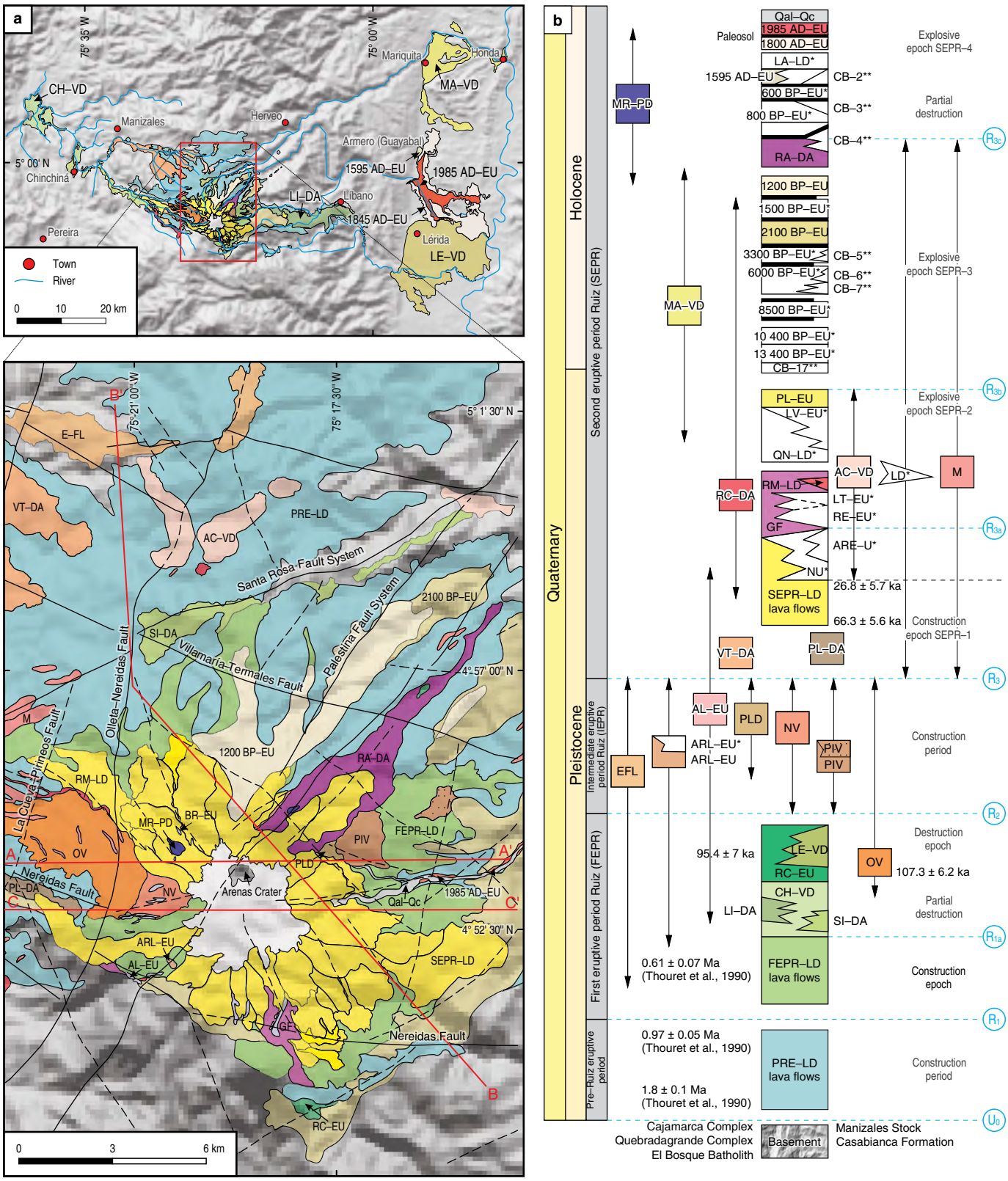

of 95.43 ± 0.7 Ma was assessed in plagioclase from a sample collected from the matrix of the RC–EU deposit (Figure 10d). The end of the destructive epoch of the FEPR is defined based on this new age.

The FEPR shows ages ranging from <0.97 Ma to 95 ka. The thick sequence of RC–EU deposits represents the destruction of the "Older Ruiz" and the possible generation of a caldera (Figure 11), which is currently covered by more recent prod-

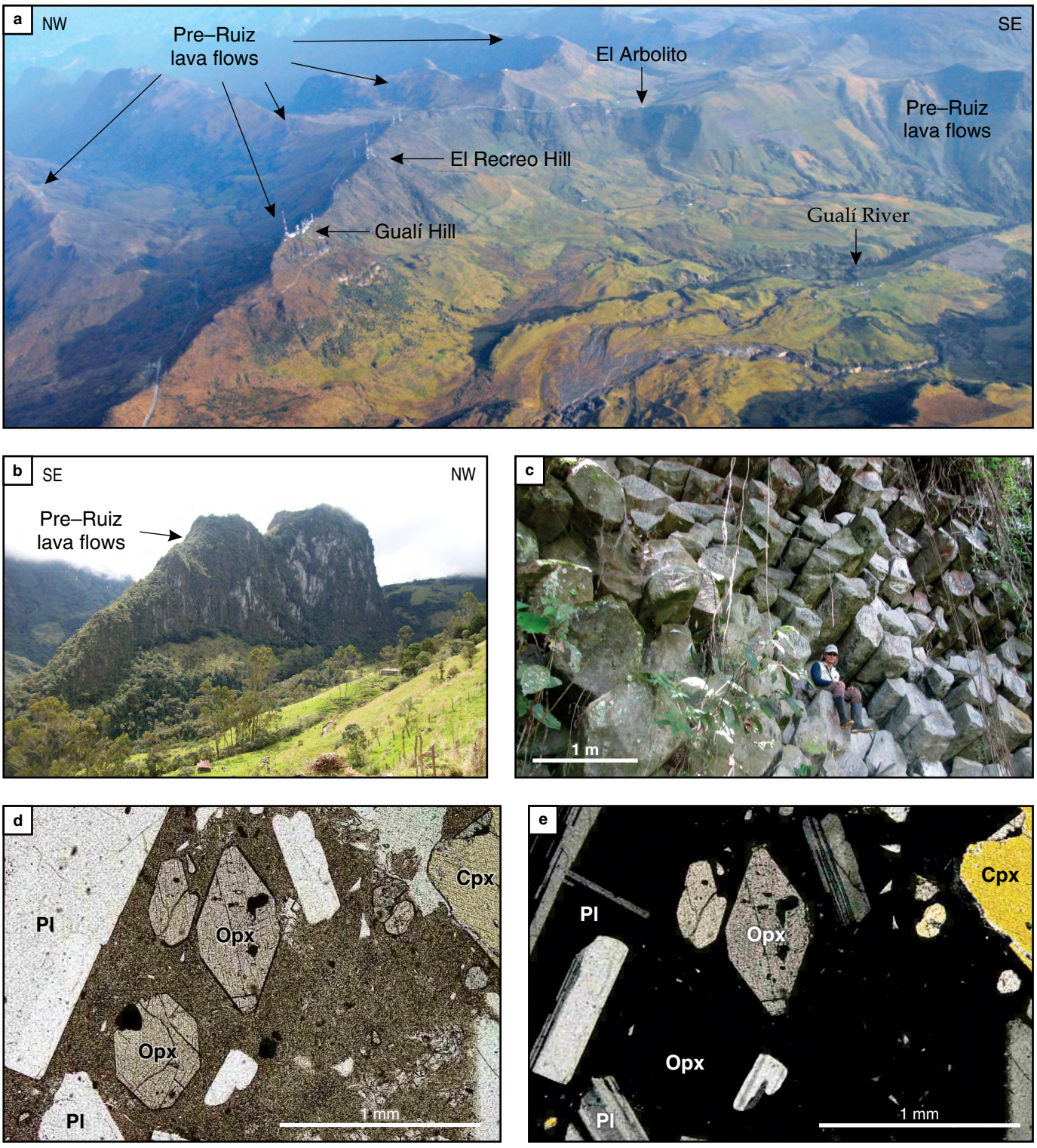

Figure 8. Pre–Ruiz eruptive period. **(a)** Aerial view N of the NRV showing the remnants of lava flows of the PRE–LD (Photograph of the OVSM, 2012). **(b)** Eroded hills of lava flows at the Recio River headwaters, S flank of the NRV. **(c)** Lava flow with columnar disjunction structures, Carros de Piedra sector, Casabianca, Tolima. **(d)** Microphotograph (taken with parallel nicols) of a lava sample collected from the N sector of the NRVC with plagioclase phenocrysts (Pl), orthopyroxene (Opx), and clinopyroxene (Cpx) in a cryptocrystalline matrix. **(e)** Microphotograph taken with crossed nicols.

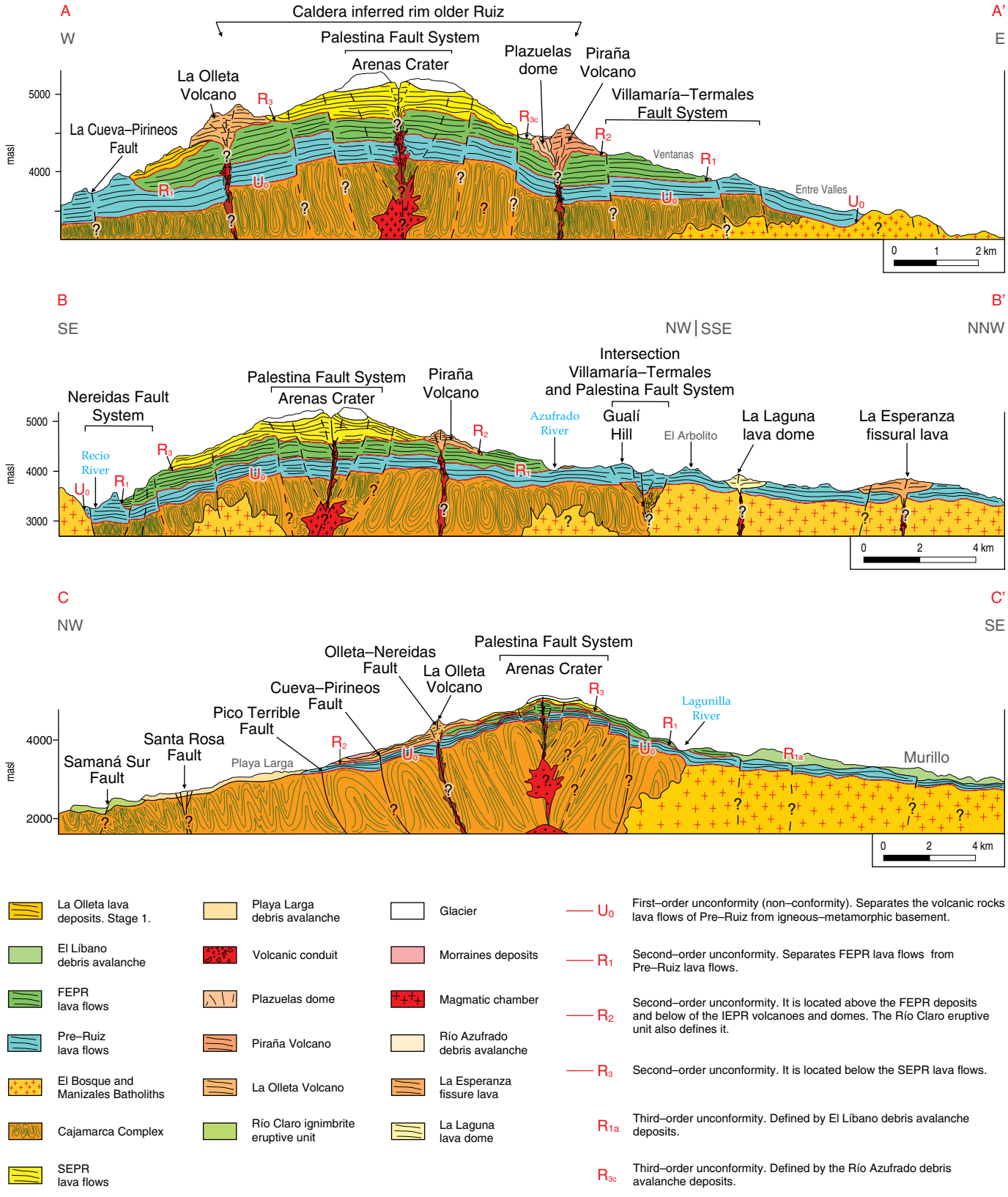

Figure 9. Schematic sections of the proximal area of the NRVC geological map. The locations are indicated in Figure 7a. The depth of the magmatic chambers is taken from Londoño & Sudo (2003). Geological profiles are based on geological interpretation and the depth data are inferred by near–surface analysis. Only the lithostratigraphic units visible at the scale of each section are represented.

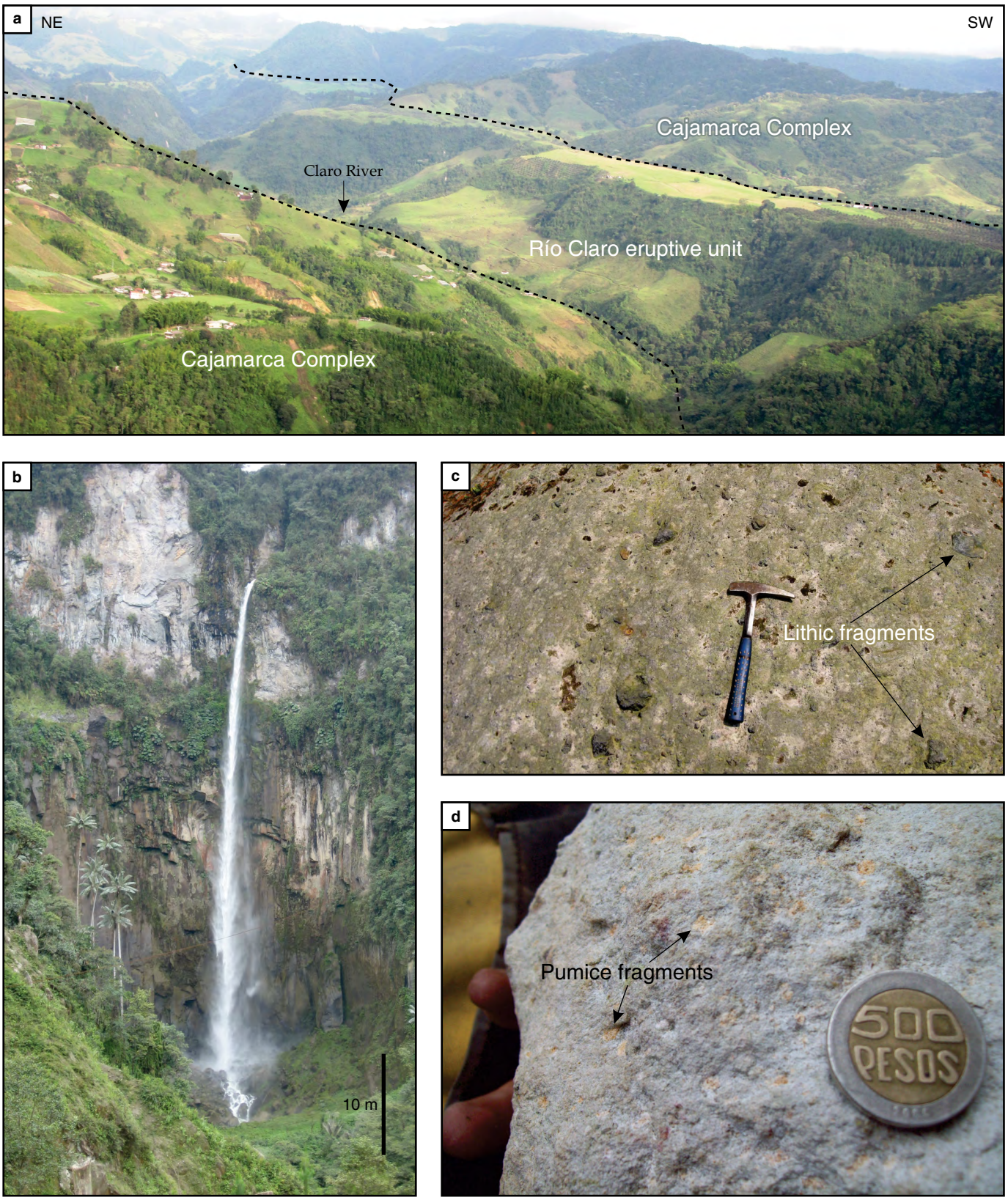

Figure 10. Río Claro eruptive unit (RC–EU). **(a)** Aerial view showing the geomorphology of the ignimbrite in contact with the Cajamarca Complex (Photograph of the OVSM, 2012). **(b)** View of the outcrop of the massif facies with columnar jointing of the RC–EU in the Nereidas abrupt ravine waterfall, Termales Botero Londoño sector. **(c)** Detail of the outcrop of the massive lithofacies, showing a supported matrix rich in lithic fragments. **(d)** Hand sample collected from the RC–EU deposit with vesicular fragments (pumice) and size ranging from lapilli to very coarse ash.

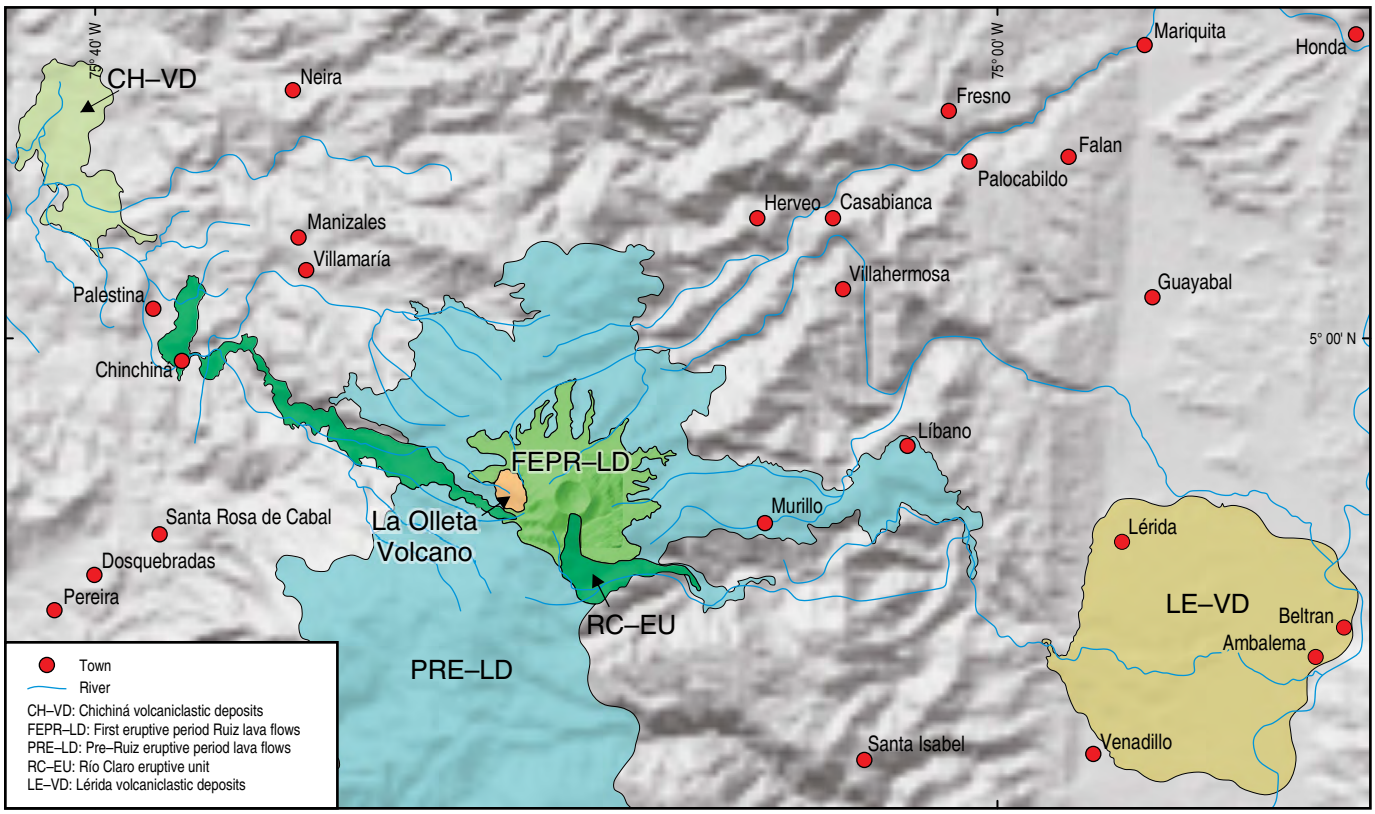

Figure 11. Reconstruction of the caldera generated during the destruction of the "Older Ruiz" volcano and associated volcanic deposits, RC–EU and LE–VD.

ucts. The deposits of this unit (Figure 10) and the surface on which they were deposited mark a second–order unconformity termed R_2 (Figure 9), which separates the "Older Ruiz" volcanic edifice from deposits from the emission centers of the Intermediate eruptive period Ruiz and the current NRV volcanic edifice. Among the R_1 and R_2 unconformities, a third–order unconformity termed R_{1a} was identified (Figure 9), and is represented by the debris avalanche deposit of El Líbano, which indicates the collapse of the E and SE flanks of the "Older Ruiz" volcano.

4.3. *Intermediate Eruptive Period Ruiz*

The Intermediate eruptive period Ruiz (IEPR) started after the destruction of the "Older Ruiz" edifice. Based on field stratigraphic relationships and geomorphological analysis, this eruptive period is interpreted to be the continuation of the construction of La Olleta Volcano and the formation of smaller volcanic centers generated near the caldera rim or intra– or extracaldera such as the Nereidas and Piraña Volcanoes, the Arenales and Alfombrales coulée domes, and the Plazuelas dome.

La Olleta Volcano was identified by Monsalve & Méndez (1997) as an adventitious volcano. Its first stage of construction began 107 ka and it continued to form during the "Intermediate eruptive period Ruiz", which was characterized by effusive volcanism and the generation of andesitic lavas. This volcano (Figure 5b) has a truncated cone shape and a semicircular crater (4850 masl) that has a collapse scar on the SW side on which different lavas flows of its second stage of generation were emplaced.

The Nereidas Volcano defined by Duque (2008) is located 2 km SW of the current NRV, has a subrounded summit (5000 masl; Figure 5d), and is formed by an assemblage of at least three lava flows that were distributed W of this eruptive center.

The Piraña Volcano (Figure 5c) is located 3.8 km E of the Arenas Crater and has very sharp and irregular geological formations at the summit (4600 masl). The edifice is formed by a lava flow distributed on the NE side of the volcano. This volcano has a PDC deposit of blocks and ash that are interpreted to represent the collapse of a dome that may have been generated at the end of the effusive activity of this volcano.

The Alfombrales dome, which is located SW of the NRV, intrudes lava flows of the "Older Ruiz". This dome is characterized by columnar disjunction structures (Figure 6b) and shows a concentrated PDC (blocks and ash flow) resulting from the partial collapse of the dome. The Arenales coulée dome outcrops SW of the NRV and has an elongated shape (Figure 6a) to the SE; the partial collapse of this dome formed a concentrated PDC (blocks and ash flow). The Plazuelas dome is located NE of the NRV, very close (Figure 6c) to the Piraña Volcano, and intrudes lava flows of the "Older Ruiz".

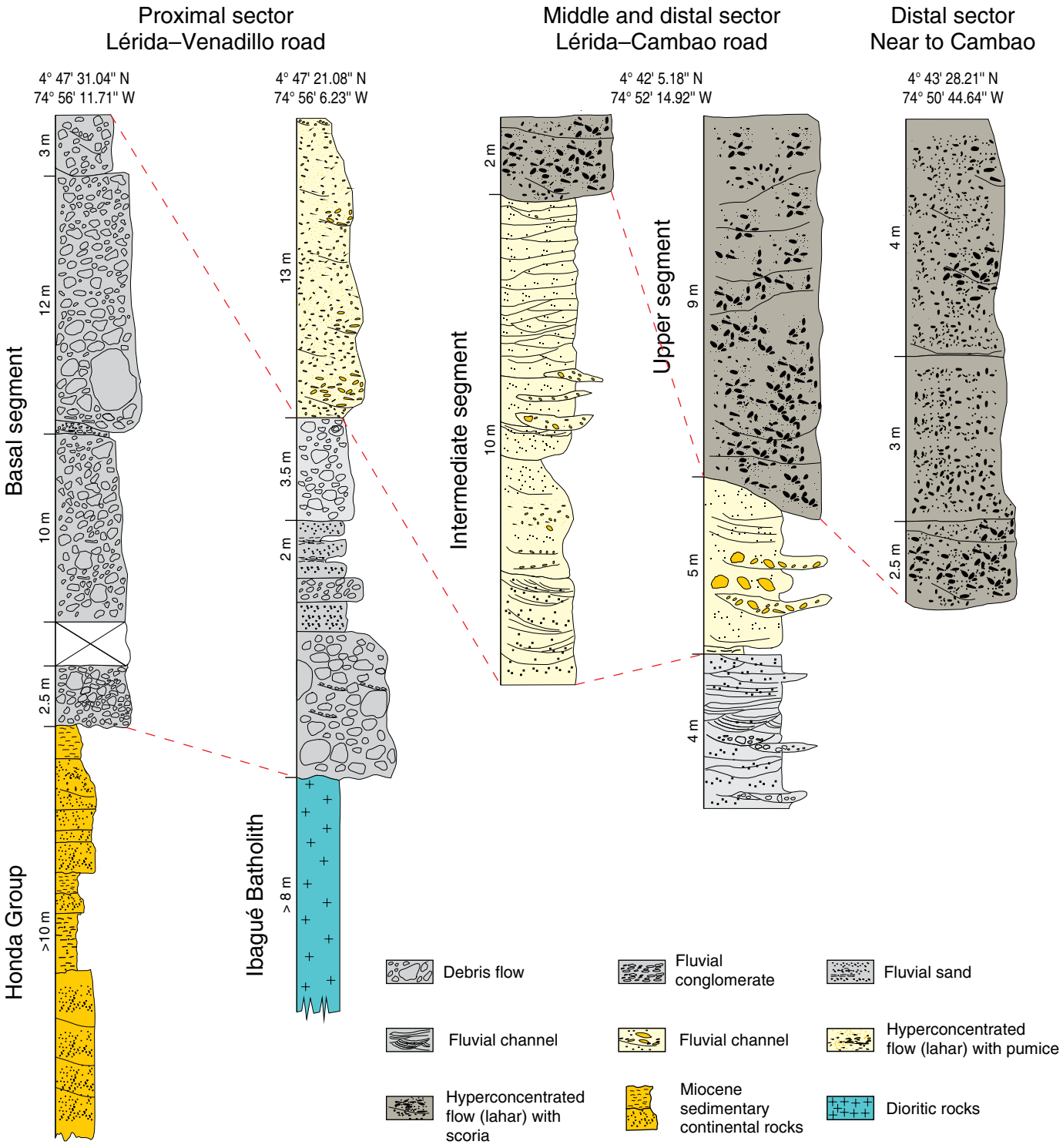

Figure 12. Stratigraphic correlation of the volcaniclastic deposits present in the Lérida Fan (LE–VD).

Compositionally, the eruptive centers of the IEPR are typically andesites with a variable content of clinopyroxene relative to orthopyroxene and variable quantities of amphibole (oxyhornblende) and biotite, both of which occur as accessory minerals.

This eruptive period occurred between the creation of the second–order unconformities R_2 and R_3 (Figure 9). R_2 separates the lava flows of the FEPR from the assemblage of domes and eruptive centers of the IEPR. This unconformity is defined by the thick sequence of deposits of PDC of the RC–EU, which indicates a stratigraphic hiatus that separates the destructive stage of the "Older Ruiz" from the subsequent construction of the eruptive centers generated during the Intermediate eruptive

period Ruiz. R_3 marks the boundary between the FEPR and the start of the construction of the NRV. The age of this eruptive period ranges from 97 to 66 ka.

4.4. Second Eruptive Period Ruiz

The construction of the NRV occurred during the Second eruptive period Ruiz (SEPR) (Figure 5a). The NRV is characterized by an initial epoch with predominantly effusive volcanism and more recent epochs with explosive eruptions.

During the initial epoch, SEPR–1, the lava flows SEPR–LD mark the start of the construction of the new volcanic edifice of the NRV. These lavas form lobes that spread radially from the NRV and are shorter and morphologically less carved by glaciers than lava flows FEPR–LD. Petrographically, these lavas are andesites with two pyroxenes and amphibole andesites. $^{40}Ar/^{39}Ar$ dating of these lava flows resulted in plateau ages of 66.3 ± 5.6 ka from the plagioclase and 26.8 ± 5.7 ka from the matrix of an andesite; these ages define the beginning of the construction of the NRV. In the proximal zone W of the NRVC, interstratified PDC were differentiated concordantly and overlie the Nereidas unit and Arenas unit lava flows, which suggests the accumulation of PDC associated with the collapse of eruptive columns. These deposits indicate temporary changes in the eruptive style from effusive to explosive eruptions, which are typical of andesitic stratovolcanoes.

This volcanism is correlated with the generation of fissural lava and an assemblage of domes that are termed the Arbolito–Curubital (Martínez et al., 2014) and the Villamaría–Termales Monogenetic Volcanic Field (Murcia et al., 2017), the volcanism of which followed the Last Glacial Maximum, from 45 to 35 ka, according to Flórez (1992). These bodies are located N of the current NRV over the Villamaría–Termales Fault System that trends NW–SE. The preserved volcanic edifices correspond to La Esperanza fissural lava deposits, La Laguna coulée dome, Santa Ana coulée dome, El Plato dome, and San Luis coulée dome (Figure 7). Petrographically, they are very different from the compositional domains observed in the effusive deposits of the NRCV, and the most typical features are increased amphibole and decreased pyroxene content and an absence of biotite. They are classified as oxyhornblendic andesites. La Esperanza fissural lava has a matrix with textures ranging from microcrystalline–microlithic to moderately intergranular, with a marked flow trend (trachytic) and with a high content of olivine microcrystals and microphenocrysts compared with the content of plagioclase; petrographically, they are classified as basaltic andesites with olivine.

The R_3 second–order unconformity (Figure 9) separates the lava flows of the SEPR–LD from the domes and volcanoes of the IEPR and marks a significant change in the eruptive style associated with the construction of the current NRV. This unconformity is physically notable in the Arenales (Figure 6a) and Alfombrales domes. Furthermore, the R_3 involves contact between the FEPR–LD rocks and the SEPR–LD rocks in several sectors (Figure 9).

Then, the explosive epoch SEPR–2 occurred in the NRV, generating primary and secondary volcaniclastic deposits. The deposits correspond to the PDC (Figure 13a–d) of the Bruma, Playa Larga, and La Vega eruptive units, and to the Molinos River pyroclastic deposits. The facies associations of these deposits indicate the generation of unstable columns during explosive eruptions, which formed concentrated and diluted PDC primarily consisting of pumice and scoria that were mainly distributed along of the Nereidas, Molinos streams, and Gualí River Basins. PDC of blocks and ash deposits, associated with the eruptive units El Plan, Las Tumbas, and Recio, suggest the highly localized accumulation of concentrated PDC (blocks and ash flows) potentially associated with the collapse of pre–existing domes, of which no remnants were identified. The ages of these deposits could not be identified; however, according to their stratigraphic relationships, these PDC were generated after the lava flows of the SEPR–LD were emplaced, which indicates that they were the result of recent explosive activity of the volcano. In addition, in an equivalent relative stratigraphic position, deposits of debris flows (lahars) outcrop in the Molinos, Nereidas upstreams and Gualí, Azufrado, Lagunilla River headwaters; the lithofacies associations of these deposits indicate successive accumulations of debris flows resulting from glacial melting by the emplacement of PDC or by the transformation and/or remobilization of volcanic materials during eruptive and posteruptive events. In the distal zone of the area of influence of the NRVC, the volcaniclastic deposits of the lower Chinchiná River Basin, the Armero sector, and the Mariquita Fan also reflect the accumulation of lahars. The Mariquita Fan contains material from both the NRVC and the Cerro Bravo Volcano.

Debris avalanche events that caused the Villamaría–Termales and Playa Larga deposits involved large rock volumes. The event that generated the Villamaría–Termales deposit is associated with three amphitheaters located in the headwaters of the Romerales, Termales, and Oliva Rivers; the deposits of this event were emplaced throughout these valleys and into the middle Chinchiná River Basin, with a total deposit volume of 2.3 km^3. The sliding event that generated the debris avalanche of the Playa Larga deposit remobilized an important section of the S and SW flanks of La Olleta Volcano, and the volume of this deposit is estimated to be 0.30 km^3. The age of these deposits is younger than the pleniglacial age of the last glaciation, which, according to Flórez (1992), was recorded in the NRV from 42 to 35 ka and is older than the pyroclastic fall sequence (CB–17 eruptive unit) of the Cerro Bravo Volcano, which, according to Lescinsky (1990), is <13 ka. The debris avalanche deposit (Figure 14) of the Azufrado River is located in the Azufrado River headwater, NE of the NRV, and its break–off scar (Figure 14a) is located 0.6 km from the center of the Arenas Crater. The

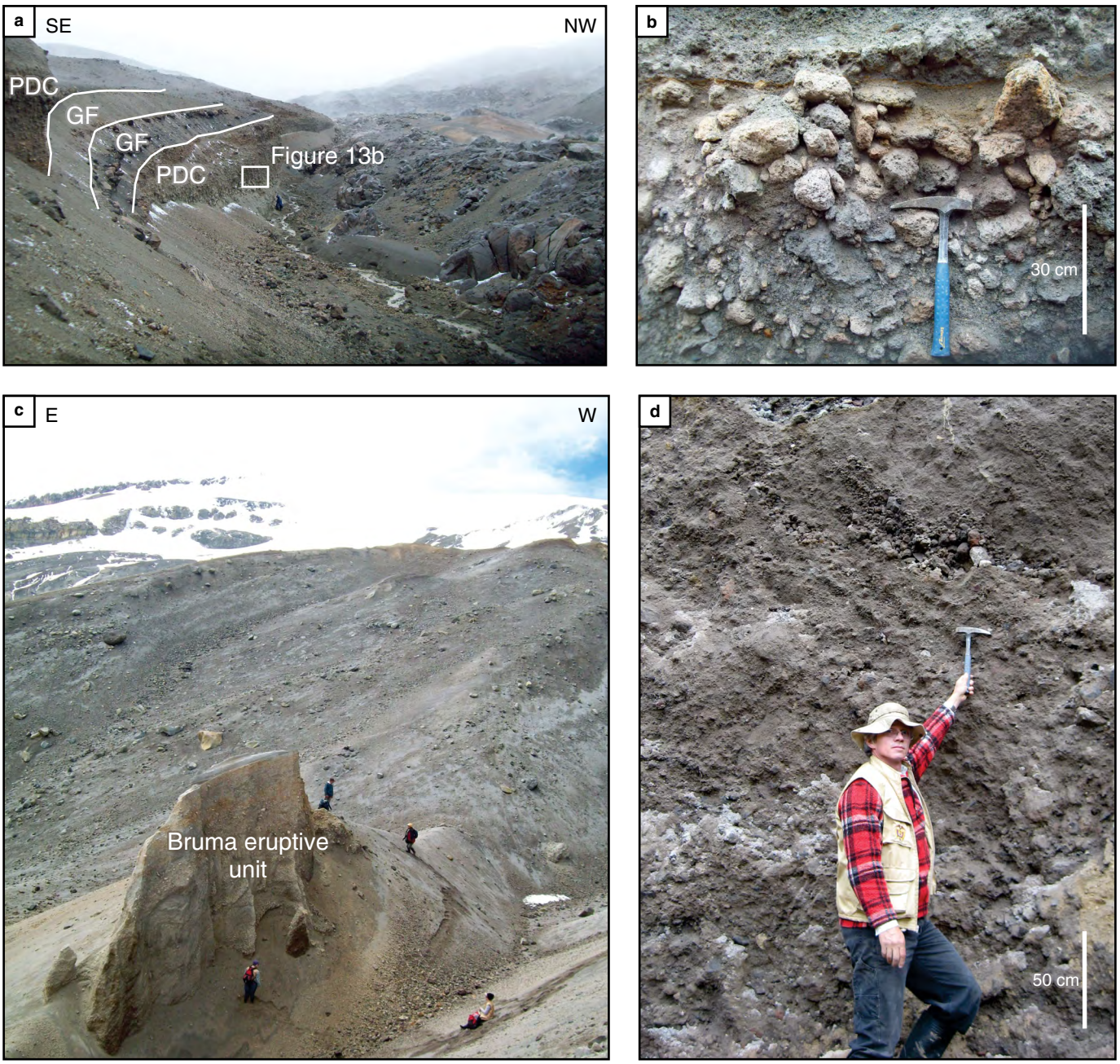

Figure 13. PDC of NRV. **(a)** View the outcrop of the MR–PD in the concentrated facies PDC interspersed with fluvioglacial deposits GF. **(b)** Detail of the outcrop of a concentrated PDC of clast–supported lithofacies with pumice. **(c)** Panoramic view of PDC of the Bruma eruptive unit on the N flank of the NRV. **(d)** Concentrated PDC with high scoria content of La Vega eruptive unit (LV–EU), outcropping in the upper section of the Nereidas abrupt ravine.

deposit (Figure 14b, 14c) has an area of 7 km^2 and a volume of 0.01 km^3, its detonator mechanism was noneruptive and it dates to between 1275 ± 50 y BP and 1595 y AD.

From approximately 13 000 y BP to recent times, a markedly explosive eruptive style occurred in the NRV, with the occurrence of several eruptive events recorded in 14 eruptive units, the ages of which were determined by ^{14}C dating (Tables 2, 3). The eruptive dynamic corresponds to eruptions with VEI ranging from 3 to 4, of subplinian character, with predominantly phreatomagmatic fragmentation styles and the generation of recurrent volcanic phenomena of PDC (Figure 15) associated with the collapse of eruptive columns, explosions and/or dome collapses, lahars (Figure 16) generated by glacier mass fusion processes, pyroclastic falls (Figure 15), and less recurrent phenomena of noneruptive debris avalanches.

Three third–order unconformities were identified above the R_3 unconformity (Figures 7, 9), which enabled the differentiation of four eruptive epochs at the end of the upper Pleistocene

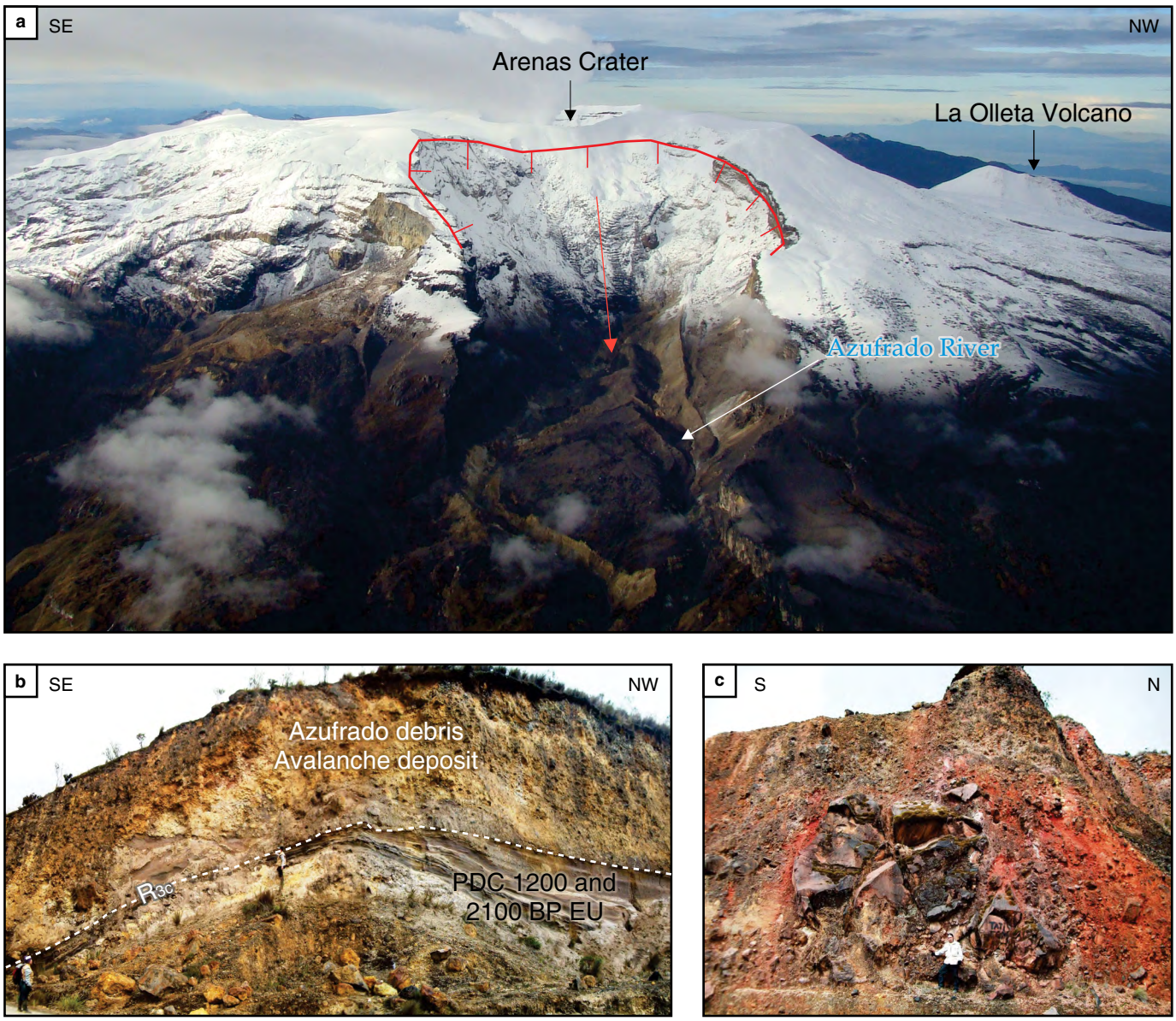

Figure 14. Flank collapse, NE zone of the NRV. **(a)** Aerial view showing the amphitheater generated by the collapse of the NE flank of the NRV in the Azufrado River headwaters (Photograph of the OVSM, 2011). **(b)** R_{3c} third–order nonconforming element defining the debris avalanche deposit. **(c)** Fragment of a block with a jigsaw structure of the debris avalanche deposit.

– Holocene in the SEPR. The unconformity R_{3a} separates the SEPR–LD lava flows from PDC, lahar and epiclastic deposits, indicating intervals with predominantly explosive origins and the remobilization of materials accumulated after the SEPR–1 eruptive epoch. The unconformity R_{3b} separates the primary volcaniclastic deposits of SEPR–2 from more restricted deposits, which, according to ^{14}C dating, date from 13 400 y BP to the present. Unconformity R_{3c} (Figure 14b) corresponds to the debris avalanche deposits of the Azufrado River. The SEPR–3 epoch from ca. 13 ka to 1275 ± 50 y BP is between the R_{3a}–R_{3b} and R_{3c} unconformities. The SEPR–4 epoch lasted from 1275 ± 50 y BP to the present and includes all volcanic deposits generated above the R_{3c} unconformity.

5. Geochemical Analysis

The major elements of the NRVC products indicate compositions ranging from basaltic andesites to dacites, with a silica content ranging from 56.37 to 69.94 % (Figure 17), a maximum alkalis ($Na_2O + K_2O$) value of 6.94%, an Al_2O_3 content ranging from 14.45 to 18.28 % (16.34% mean), and mean and maximum values of MgO of 3.40% and 8.56%, respectively. Most major elements, CaO, MgO, FeO, Fe_2O_3, TiO_2, and MnO show typical negative correlations with the increase in SiO_2, indicating magmatic differentiation, except for K_2O, which shows a positive correlation, and Na_2O, Al_2O_3, and P_2O_5, which are relatively scattered. The K_2O content (ranging from 1.16 to 3.12 %)

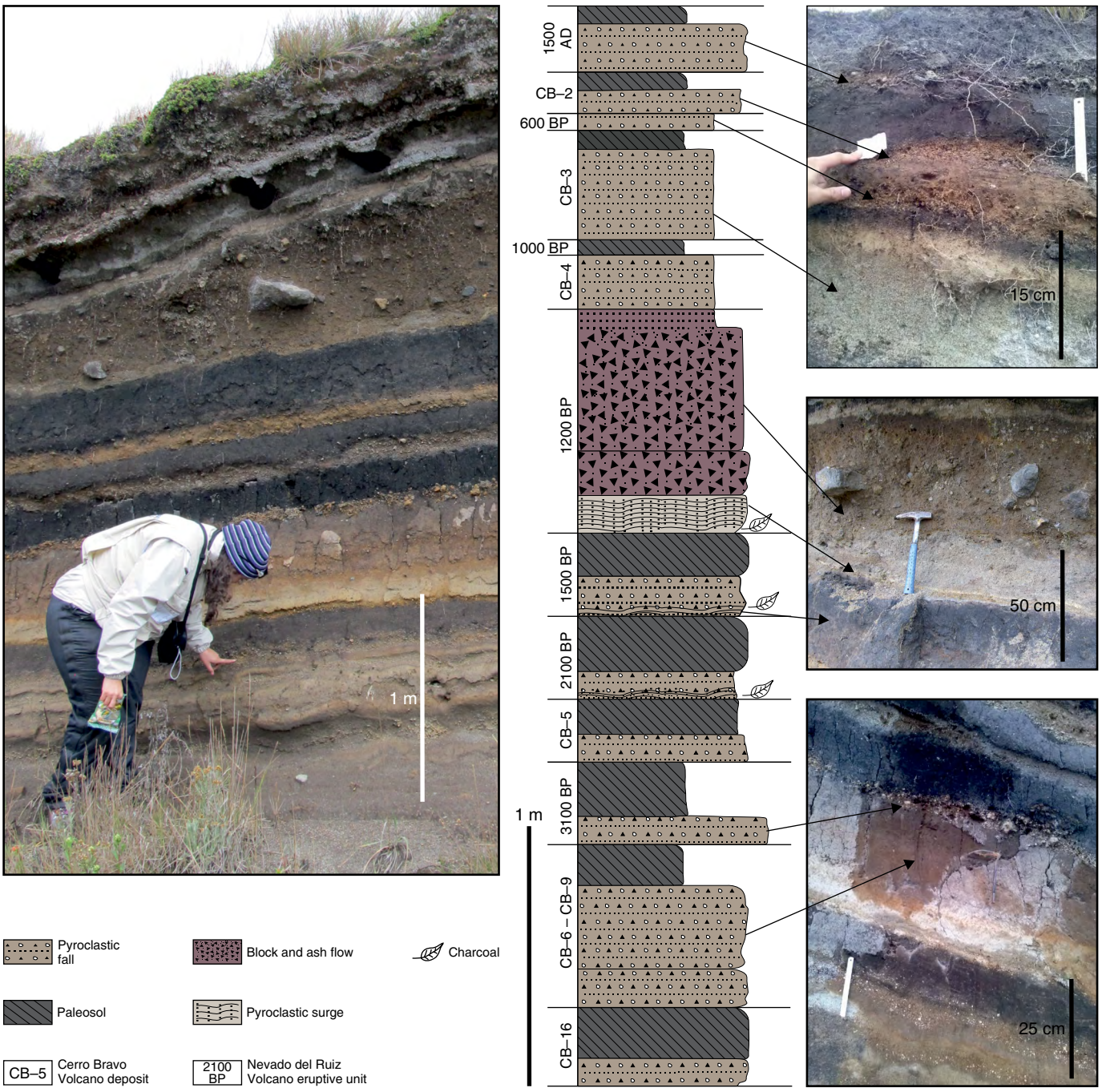

Figure 15. Pyroclastic fall deposits and PDC of the most recent explosive activity of the NRV. The CB correspond to pyroclastic fall deposits of the Cerro Bravo Volcano.

clearly increases as the SiO_2 content increases. In general, this behavior is typical of calc–alkaline rocks (Figure 18) associated with subduction zones of active continental margins (Bailey, 1981; Bryant et al., 2006; Gill, 1981).

Trace elements, such as Rb, Ba, Sr, and Cs, especially Rb and Ba, from the group of low field strength elements (LFSEs), show positive correlations with SiO_2, whereas Sr and Cs are relatively scattered. High field strength elements (HFSEs), represented by U, Th, and Pb, show positive correlations with SiO_2, but this relationship is weakest for Pb. The HFSEs, such as Sc, Co, V, Zn, Cr, and Ni (transition metals), are negatively correlated with SiO_2.

Primitive mantle–normalized low–field strength elements show highly irregular behaviors, with very marked peaks and depressions, and are very parallel to each other, with a decreasing trend in enrichment degree in the large–ion lithophile elements (LILEs; Cs, Rb, and Ba), the Th–U pair and the heavy rare earth elements (HREEs; Yb and Lu); in addition, there is a marked

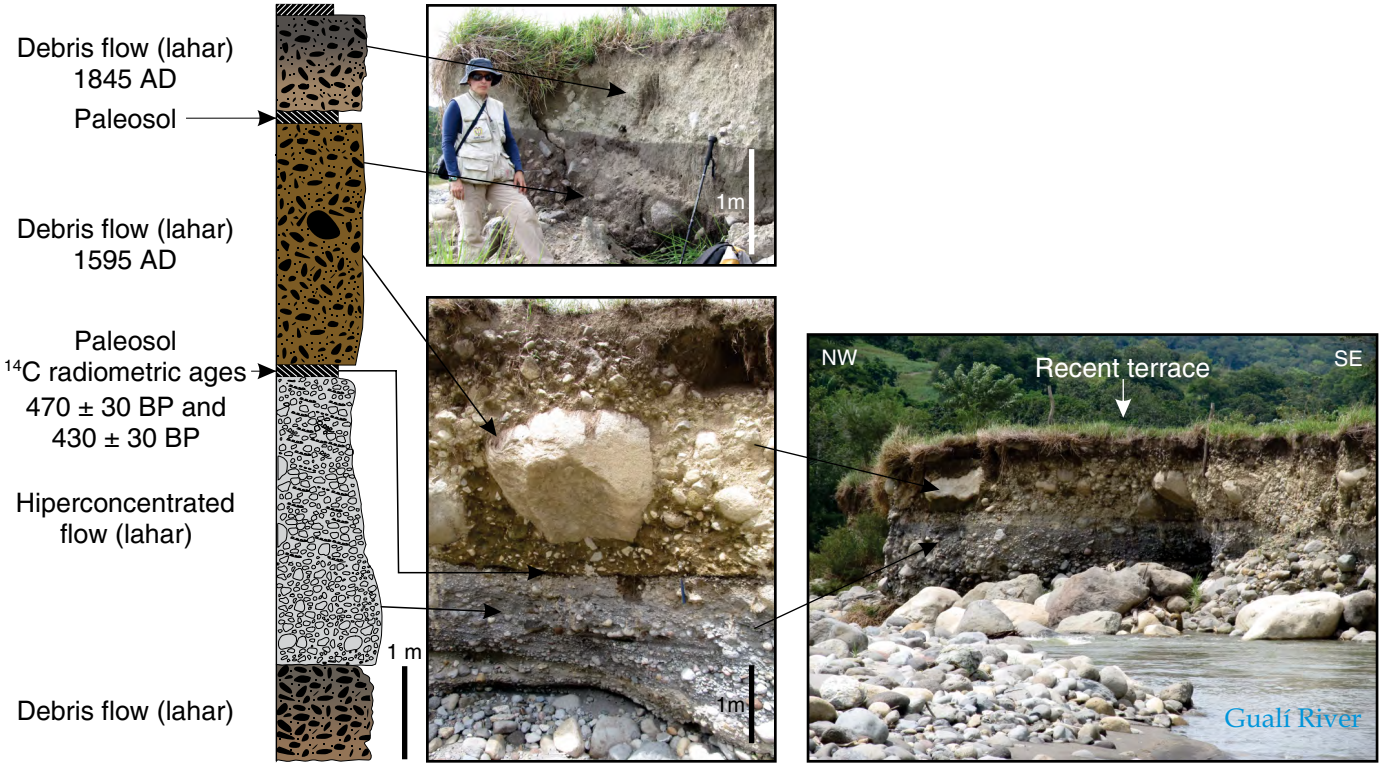

Figure 16. Lahar deposits associated with the NRV in the lower section of the Gualí River, between the municipalities of Mariquita and Honda, Tolima Department.

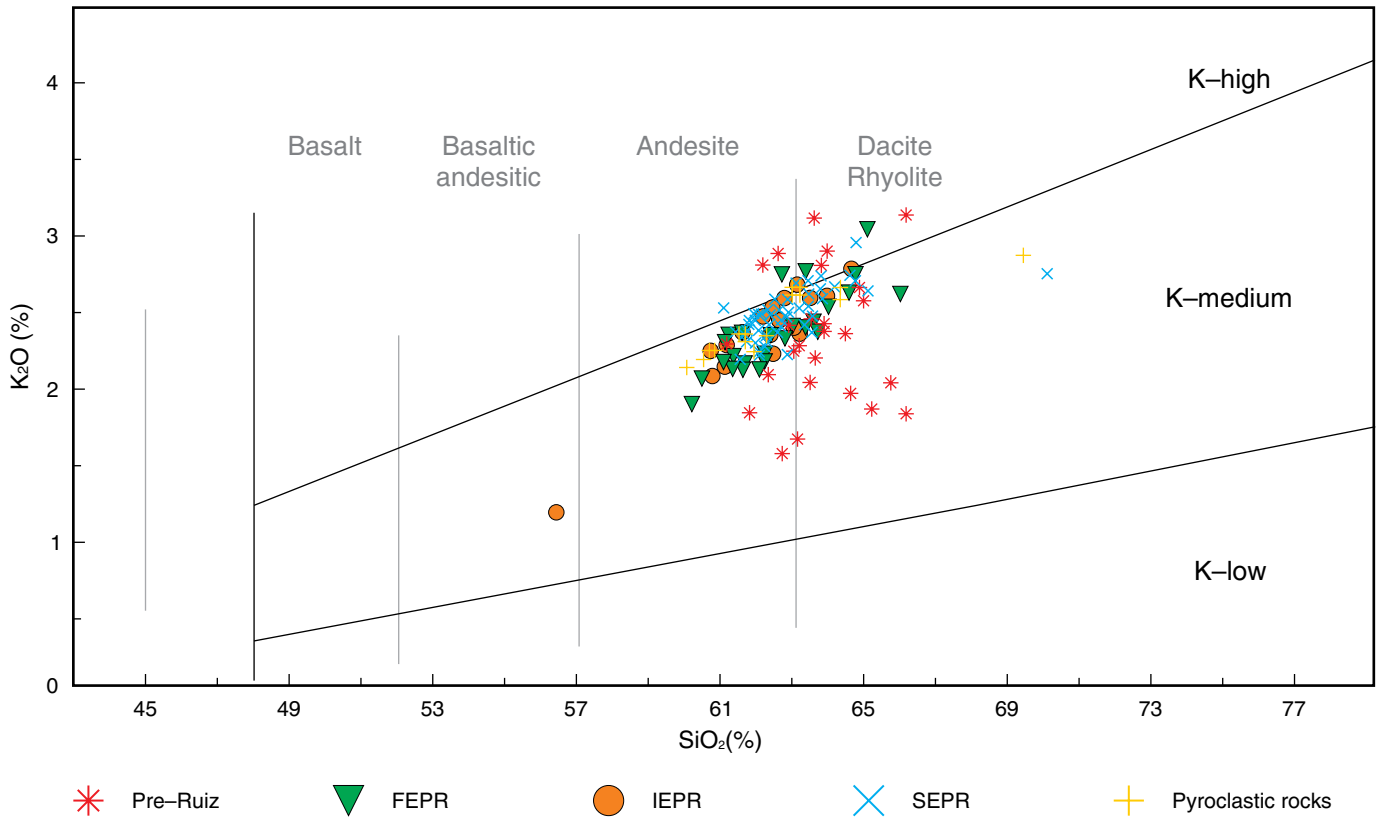

Figure 17. SiO_2 vs. K_2O diagram of the IUGS with samples representative of the NRVC.

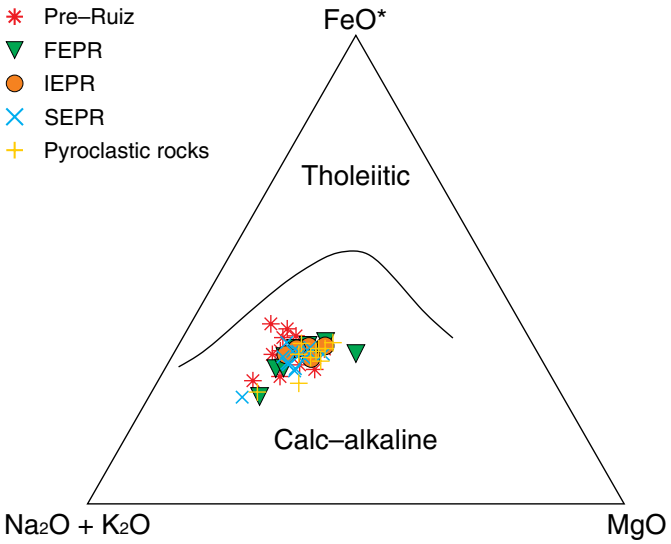

Figure 18. AFM diagram (Na_2O + K_2O, FeO*, and MgO; Irvine & Baragar, 1971) in which the representative samples of the NRVC have been graphed.

positive Pb anomaly, minor positive Ba, U, Sr, Zr, and Tb anomalies, and a few minor P and Ti depressions. This pattern is consistent for most samples, which also show an increased enrichment in LILEs, LREEs, and HFSEs, and a clear decreased enrichment in MREEs, HREEs, and Ti. The positive Pb, Sr, and Zr anomalies may be caused by crustal contamination (Rudnick & Gao, 2003). The positive Ba peaks indicate a contribution from the subduction plate. The increased enrichment in more mobile low–field strength elements, such as Ba, Rb, and Cs, would indicate the contribution of added components to the mantle source through fluids coming from the subduction zone, similarly indicating increased differentiation of the derived magmas by fractional crystallization with respect to the magma generated in the primary source by partial melting (Rudnick & Gao, 2003).

Drummond & Defant (1990) introduced the term adakite to indicate "volcanic or intrusive rocks in Cenozoic arcs associated with young oceanic lithosphere subduction (≤25 Ma)". Several samples from different eruptive periods identified in the NRVC show an adakitic trend (Figure 19). The geochemical behaviors of specific trace elements and REEs in several samples indicate clear adakitic indicators, such as high Sr concentrations (from 518 to 848 ppm), low HREEs concentrations (Yb ranging from 1.09 to 1.96 ppm), and Y values ranging from 10.4 to 18.7 ppm, high values of the Sr/Y ratio (from 33.06 to 72.60), and a marked enrichment in LREEs and LILEs and strongly fractionated REEs patterns.

6. Discussion

In this study, 52 lithostratigraphic units were identified and 23 could be defined as eruptive units limited at their base and top by paleosols, which denote a time of rest in volcanic activity or, at least, a time during which the eruptive activity left no geological record. A U_0 first–order unconformity, which separates the volcanic deposits of the NRVC from the basement, and three larger second–order unconformities (R_1, R_2, and R_3), which cover the entire NRVC and indicate abrupt changes in the sequence of eruptive products, denoting significant changes in the volcano–magmatic system, were identified. The third–order unconformities (R_{1a}, R_{3a}, R_{3b}, and R_{3c}) only cover part of the volcanic edifices and mark key changes in the system (for example, the debris avalanches and the thick fluvioglacial sequences indicate mass destruction and removal of much of the edifice involved). Thus, minor unconformities are reflected by the presence of paleosols that cover only several areas and/or sectors of the NRVC, which were therefore only used for local correlations and for defining eruptive units. Those discontinuities produced by syn–sedimentary erosive processes or associated with transport mechanisms were disregarded when defining a subdivision of the volcanic stratigraphy.

The Pre–Ruiz eruptive period corresponds to the construction of the "Ancestral Ruiz" volcano and encompasses all deposits accumulated between the unconformity U_0 (which defines the limit with the basement), and the unconformity R_1; K/Ar ages ranging from ca. 1.8 to 0.97 Ma assessed by Thouret et al. (1990) are known for this period of predominantly effusive activity. Furthermore, the absence of ignimbrites in the NRVC below unconformity R_1 implies that neither the formation of a caldera hypothesized by Thouret et al. (1990) at the end (0.97–0.76 Ma) of the "Ancestral Ruiz", nor their hypothesis that the presence of the Gualí and Arbolito domes resulted from the resurgent activity of the caldera, could be validated in the present study. The Gualí and Arbolito Hills are interpreted to be remnants of the "Ancestral Ruiz" volcano.

The First eruptive period Ruiz, which includes all deposits accumulated between unconformities R_1 and R_2, began with a constructive epoch of the "Older Ruiz", which was followed by a destructive epoch that culminated with the evacuation of part of the magmatic reservoir, deposition of the RC–EU, and formation of a caldera. Thouret et al. (1990) proposed an age of 0.76 ± 0.05 Ma (K/Ar) for the start of the constructive epoch; the location of the sample was revised, establishing that it belongs to the low section of a lava flows of the Santa Isabel Dome Complex; therefore, this age should not be assumed as the start of this eruptive period. Alternatively, the proposed start would be earlier than 0.97 Ma. The Río Claro Ignimbrite, which was identified by Grand & Handszer (1989), and dated to 0.2 ± 0.07 Ma by Thouret et al. (1990) was redefined in this study as the RC–EU, with a calculated volume of approximately 5 km^3, a mean thickness of 200 m, and an area of 25 km^2, disregarding the volumes that could have been eroded and the volumes of the fall deposits associated with such a unit. $^{40}Ar/^{39}Ar$ dating indicated that the plateau age in the plagioclase of the RC–EU was 95.43 ± 0.7 ka, which allows the end of this eruptive pe-

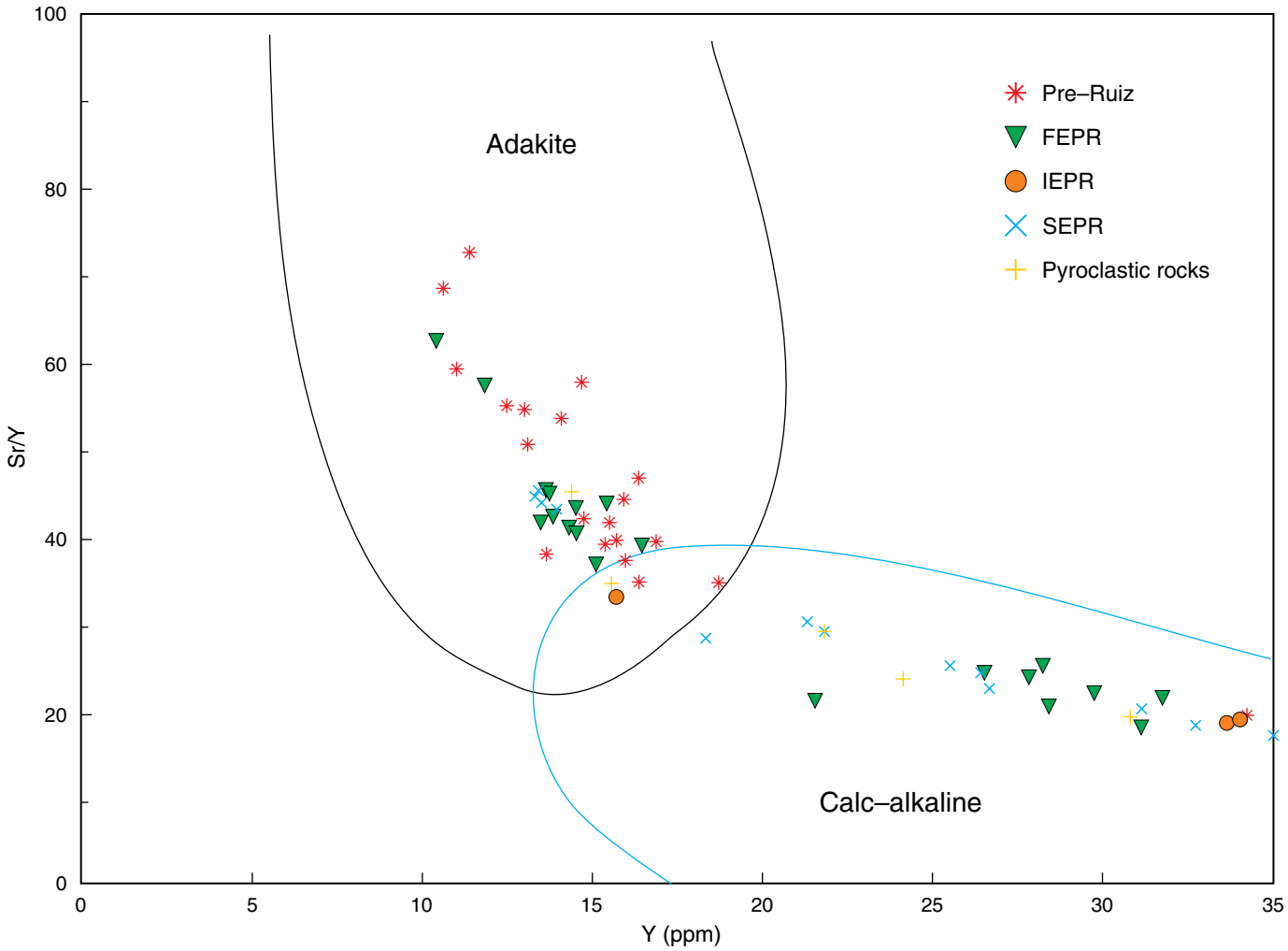

Figure 19. Y vs. Sr/Y diagram (retrieved and modified from Drummond & Defant, 1990) discriminating adakites from the "typical" calc–alkaline rocks on which data on samples from the NRVC are plotted.

riod to be determined. According to Geyer & Martí (2009), the formation of a caldera indicates a dramatic change in the magmatic–volcanic system and requires a sufficiently long time for its reconfiguration, which compromises the establishment of a new reservoir. The unconformity R_2 was defined according to the recommendations by Lucchi (2013), who established the identification of calderas and associated ignimbrites; in this case, the caldera formed at the end of this eruptive period and its associated ignimbrite deposits RC–EU were used as stratigraphic markers to identify the second–order unconformity.

The NRCV is emplaced at the intersection between the south section of the Palestina Fault System (strike–slip faults with right–lateral transcurrent motions and NE–SW directions; Mejía et al., 2012), which has strike–slip structures with normal movement, and the NW–SE direction, among which the Villamaría–Termales Fault System stands out (Bohórquez et al., 2005; González & Jaramillo 2002; Thouret et al., 1990). These structures and the current tectonic stress field (Toro & Osorio, 2005) favor the development of fracturing in the area of the NRVC; this fracturing likely controls the differential emplacement, the distribution and transit of magmas, and the development of feeder conduits for different eruptive sources of the NRVC. Londoño & Sudo (2003) proposed that these structures intersected two magmatic chambers located at a depth between 3 and 8 km below the current NRV. Within the exposed tectonic framework, volcanism generated by the NRVC has been primarily andesitic to dacitic (occasionally with basaltic andesites and dacites), of calc–alkaline affinity, and with a medium to high K_2O content. Fractional crystallization would explain the compositional variations throughout the magmatic evolution of the NRVC without ruling out the participation of other mechanisms such as crustal assimilation/contamination and magma mixing, as mentioned by Ancochea et al. (1991), Calvache (1990), Central Hidroeléctrica de Caldas S.A. (1983), Gourgaud & Thouret (1990), Jaramillo (1980), Melson et al. (1990), Schaefer (1995), Sigurdsson et al. (1990), Thouret et al. (1985, 1990), Vatin–Pérignon et al. (1990), and Young (1991). In general, the volcanism of the NRVC shows a compositional continuous trend which the composition of the

products formed during the different eruptive periods ranges from more basic andesites to dacitic rocks. This behavior may be due to recurrent recharges with more basic magmas from reservoirs located in deeper levels of the crust (perhaps at >10 km considering the stability of the olivine) towards shallower magmatic chambers (possibly at <10 km). Adakitic geochemical trend of some samples identified in the NRVC requires more detailed studies to determine their origin.

According to the interpretation of the geological record and the eruptive dynamics, the NRV corresponds to a volcano composite of andesitic composition, with an age of 66 ka BP. In the last 13 000 years, the volcano has been characterized by predominantly explosive activity, with a VEI between 3–4 and a subplinian style, with the record of at least fourteen (14) pulses and eruptive phases. Historically, eruptive events occurred on the years 1595, 1800–1845, and 1985 AD. This information is fundamental for the assessment of the volcanic hazard and as a support for the management of volcanic risk.

7. Conclusions

The geological evolution of the NRVC has been established following updated international criteria for volcano geology. The integration of field data with results from geomorphological, petrographic, geochemical, and radiometric analyses revealed four main eruptive periods during the evolution of the complex over the past 1.8 my.

The NRVC is divided into four eruptive periods: (1) the Pre–Ruiz eruptive period from 1.8 ± 0.1 Ma to 0.97 ± 0.05 Ma includes one or several eruptive centers of effusive domain; (2) the First eruptive period Ruiz, estimated to have started prior to 0.97 Ma, continued until approximately 95.43 ± 0.7 ka; this period was initially dominated by effusive eruptions, followed by a highly explosive destructive epoch, which culminated with the partial evacuation of the magmatic reservoir and the formation of a caldera; (3) the Intermediate eruptive period Ruiz, during which domes and volcanoes of intracaldera rims and/or extracaldera volcanoes with ages ranging from 95.43 ± 0.7 ka to 66.3 ± 5.6 ka were formed; and (4) the Second eruptive period Ruiz, which started at 66.3 ± 5.6 ka and continues today and corresponds to the current NRV, which has demonstrated a markedly explosive behavior during the last 13 ka and has generated recurrent lahars, PDC, and pyroclastic falls and less recurrent noneruptive debris avalanches.

A first–order unconformity, U_0, was identified and separates the volcanic deposits of the NRVC from the (igneous–metamorphic) basement. The second–order unconformities (R_1, R_2, and R_3) mark the separation of the three main volcanic edifices, indicating significant changes in the volcano–magmatic system. The first edifice, "Ancestral Ruiz", corresponds to one or several emission centers. The second edifice, "Older Ruiz", was initially constructed during a time of effusive eruptions, continuing with the same eruptive style as that of the "Ancestral Ruiz", and was followed by a highly explosive, destructive epoch, which culminated with the evacuation of part of the magmatic reservoir and the formation of a caldera. The third main edifice, the NRV, corresponds to the current stratovolcano. Third–order unconformities (R_{1a}, R_{3a}, R_{3b}, and R_{3c}) affect part of the volcanic edifices and indicate key changes, such as the occurrence of debris avalanches.

The NRVC rocks are of calc–alkaline character, have a medium to high K_2O content, and are associated with a subduction zone of an active continental margin. The magmas apparently result from a combination of processes of partial fusion of the asthenospheric wedge, previously metasomatized by fluids derived from the subduction plate, fractional crystallization, contamination or crustal assimilation, and magma mixing.

Acknowledgments

The authors of the present study express their gratitude for the valuable support of the technical and operational staff of the Observatorios Vulcanológicos y Sismológicos de Manizales y Popayán of the SGC, especially to Gloria Patricia CORTÉS and Adriana AGUDELO, and the headquarters of the SGC in Bogotá, particularly to Marta Lucía CALVACHE and Alberto OCHOA. The authors also thank Natalia PARDO–VILLAVECES for valuable thematic contributions and the inhabitants of the region of the NRV for their kind help and company during the long field trips made by the geologists.

References

Aguirre, O.R. & López, J.A. 2003. Cartografía geológica y petrografía del Stock de Manizales y su relación con sus rocas encajantes. Manizales, Colombia. Bachelor thesis, Universidad de Caldas, 194 p. Manizales.

Ancochea, E., Borrero, C.A., Fuster, J.M. & Naranjo, J.L. 1991. Geoquímica de las lavas antiguas del Volcán del Ruiz, Colombia, sector noroccidental. Simposio sobre magmatismo andino y su marco tectónico. Memoirs, I, p. 65–76. Manizales.

Aristizabal, M. & Echeverry, L.M. 2001. Volcán Tesorito, geología detallada a escala 1:2000 y modelo evolutivo. Bachelor thesis, Universidad de Caldas, 76 p. Manizales.

Ayala, L.F. 2009. Petrografía y modelo vulcanológico del Volcán Nevado del Ruiz Etapa Ancestral. Bachelor thesis, Universidad de Caldas, 113p. Manizales.

Bailey, J.C. 1981. Geochemical criteria for a refined tectonic discrimination of orogenic andesites. Chemical Geology, 32(1–4): 139–154. https://doi.org/10.1016/0009–2541(81)90135–2

Bohórquez, O.P., Monsalve, M.L., Velandia, F., Gil, F. & Mora, H. 2005. Marco tectónico de la cadena volcánica más septentrional de la cordillera Central de Colombia. Boletín de Geología, 27(1): 55–79.

Borrero, C.A. & Naranjo, J.L. 1990. Casabianca Formation: A Colombian example of volcanism–induced aggradation in a fluvial basin. Journal of Volcanology and Geothermal Research, 41(1–4): 253–267. https://doi.org/10.1016/0377–0273(90)90091–S

Borrero, C.A., Toro, L.M., Alvarán, M. & Castillo, H. 2009. Geochemistry and tectonic controls of the effusive activity related with the Ancestral Nevado del Ruiz Volcano, Colombia. Geofísica Internacional, 48(1): 149–169.

Bourdon, E., Eissen, J.P., Gutscher, M.A., Monzier, M., Hall, M.L. & Cotten, J. 2003. Magmatic response to early aseismic ridge subduction: The Ecuadorian margin case, South America. Earth and Planetary Science Letters, 205(3–4): 123–138. https://doi.org/10.1016/S0012–821X(02)01024–5

Brook, M. 1984. New radiometric age data from SW Colombia. Ingeominas–Misión Británica, unpublished report 10, 25 p. Cali.

Bryant, J.A., Yogodzinski, G.M., Hall, M.L., Lewicki, J.L. & Bailey, D.G. 2006. Geochemical constraints on the origin of volcanic rocks from the Andean Northern Volcanic Zone, Ecuador. Journal of Petrology, 47(6): 1147–1175. https://doi.org/10.1093/petrology/egl006

Calvache, M.L. 1990. Pyroclastic deposits of the November 13, 1985 eruption of Nevado del Ruiz Volcano, Colombia. Journal of Volcanology and Geothermal Research, 41(1–4): 67–78. https://doi.org/10.1016/0377–0273(90)90083–R

Central Hidroeléctrica de Caldas S.A. 1983. Investigación geotérmica Macizo Volcánico del Ruiz: Geovulcanología. Fase II, Etapa A, III, 94p. Bogotá.

de Silva, S.L. & Francis, P.W. 1991. Volcanoes of the Central Andes. Springer, 216 p. Berlin, Heidelberg, Germany.

Drummond, M.S. & Defant, M.J. 1990. A model for trondhjemite–tonalite–dacite genesis and crustal growth via slab melting: Archean to modern comparisons. Journal of Geophysical Research: Solid Earth, 95(B13): 21503–21521. https://doi.org/10.1029/JB095iB13p21503

Duque, D.M. 2008. Caracterización de una estructura volcánica ubicada al SW del Cráter Arenas–Volcán Nevado del Ruiz. Bachelor thesis, Universidad de Caldas, 64 p. Manizales.

Feininger, T., Barrero, D. & Castro, N. 1972. Geología de parte de los departamentos de Antioquia y Caldas (sub–zona II–B). Boletín Geológico, 20 (2): 1–173.

Fisher, R.V. & Schmincke, H.U. 1984. Pyroclastic rocks. Springer–Verlag, 472 p. Berlin, Heidelberg, Germany. https://doi.org/10.1007/978–3–642–74864–6

Flórez, A. 1986. Geomorfología del área Manizales–Chinchiná, cordillera Central, Colombia. Instituto Geográfico Agustín Codazzi, 158 p. Bogotá.

Flórez, A. 1992. Los nevados de Colombia: Glaciales y glaciaciones. Análisis Geográficos, (22): p. 1–95

Gansser, A. 1973. Facts and theories on the Andes: Twenty–sixth William Smith Lecture. Journal of the Geological Society, 129: 93–131. https://doi.org/10.1144/gsjgs.129.2.0093

Geyer, A. & Martí, J. 2009. Stress fields controlling the formation of nested and overlapping calderas: Implications for the understanding of caldera unrest. Journal of Volcanology and Geothermal Research, 181(3–4): 185–195. https://doi.org/10.1016/j.jvolgeores.2009.01.018

Gill, J. 1981. Orogenic andesites and plate tectonics. Springer–Verlag. 392 p. Berlin. https://doi.org/10.1007/978–3–642–68012–0

Gómez, J., Montes, N.E., Nivia, Á. & Diederix, H., compilers. 2015. Geological Map of Colombia 2015. Scale 1:1 000 000. Servicio Geológico Colombiano, 2 sheets. Bogotá. https://doi.org/10.32685/10.143.2015.936

González, H. 1989. Análisis de la nomenclatura estratigráfica de las rocas metamórficas (Litodema A), al este del límite oriental de la zona de Falla de Romeral, cordillera Central, Colombia. Ingeominas, unpublished report, 21 p. Medellín.

González, L. & Jaramillo, C.M. 2002. Estudio neotectónico multidisciplinario aplicado a la Falla Villamaría–Termales. Bachelor thesis, Universidad de Caldas, 168 p. Manizales.

Gourgaud, A. & Thouret, J.C. 1990. Magma mixing and petrogenesis of the 13 November 1985 eruptive products at Nevado del Ruiz, Colombia. Journal of Volcanology and Geothermal Research, 41(1–4): 79–96. https://doi.org/10.1016/0377–0273(90)90084–S

Grand, M.M. & Handszer, A. 1989. Naturaleza y dinámica de un flujo piroclástico en la zona de Nereidas. Bachelor thesis, Universidad de Caldas, 175 p. Manizales.

Groppelli, G. & Viereck–Goette, L., editors. 2010. Stratigraphy and geology of volcanic areas. The Geological Society of America, Special Paper 464, 294 p. https://doi.org/10.1130/SPE464

Herd, D.G. 1974. Glacial and volcanic geology of the Ruiz–Tolima Volcanic Complex, Cordillera Central, Colombia. Doctorade thesis, University of Washington. 77p. Seattle, USA.

Herrera, J.S. & López, S.A. 2003. Estratigrafía de la Formación Manizales y propuesta de un modelo de depósito. Bachelor thesis, Universidad de Caldas, 91 p. Manizales.

Hobden, B.J., Houghton, B.F., Lanphere, M.A. & Nairn, I.A. 1996. Growth of the Tongariro Volcanic Complex: New evidence from K–Ar age determinations. New Zealand Journal of Geology and Geophysics, 39(1): 151–154. https://doi.org/10.1080/00288306.1996.9514701

Irvine, T.N. & Baragar, W.R.A. 1971. A guide to the chemical classification of the common volcanic rocks. Canadian Journal of Earth Sciences, 8(5): 523–548. https://doi.org/10.1139/e71-055

Jaramillo, J.M.J. 1980. Petrology and geochemistry of the Nevado del Ruiz Volcano, northern Andes, Colombia. Doctorade thesis, University of Houston, 183 p. Houston, USA.

Lescinsky, D.T. 1990. Geology, volcanology, and petrology of Cerro Bravo, a young dacitic, stratovolcano in west–central Colombia. Master thesis, Louisiana State University, 182 p. Baton Rouge, USA.

Londoño, J.M. & Sudo, Y. 2003. Velocity structure and a seismic model for Nevado del Ruiz Volcano, Colombia. Journal of Volcanology and Geothermal Research, 119(1–4): 61–87. https://doi.org/10.1016/S0377–0273(02)00306–2

Lucchi, F. 2013. Stratigraphic methodology for the geological mapping of volcanic areas: Insights from the Aeolian Archipelago (southern Italy). Geological Society of London, Memoirs 37, p. 37–53. London. https://doi.org/10.1144/M37.5

Martí, J., Groppelli, G. & Brum da Silveira, A. 2018. Volcanic stratigraphy: A review. Journal of Volcanology and Geothermal Research. 357: 68–91. https://doi.org/10.1016/j.jvolgeores.2018.04.006

Martínez, L.M., Valencia, L.G., Ceballos, J.A., Narváez, B.L., Pulgarín, B.A., Correa, A.M., Navarro, S., Murcia, H.F., Zuluaga, I., Rueda, J.B. & Pardo, N. 2014. Geología y estratigrafía del Complejo Volcánico Nevado del Ruiz. Servicio Geológico Colombiano, unpublished report, 403 p. Bogotá.

Meissner, R., Flueh, E.R. & Muckelmann, R. 1980. Sobre la estructura de los Andes septentrionales: Resultados de investigaciones geofísicas. In: Nuevos resultados de la investigación geocientífica alemana en Latinoamérica. Deutsche Forschungsgemein–Schaft, p. 79–90. Bonn.

Mejía, E.L., Velandia, F., Zuluaga, C.A., López, J.A. & Cramer, T. 2012. Análisis estructural al noreste del Volcán Nevado del Ruíz, Colombia: Aporte a la exploración geotérmica. Boletín de Geología, 34(1): 27–41.

Melson, W.G., Allan, J.F., Jerez, D.R., Nelen, J., Calvache, M.L., Williams, S.N., Fournelle, J. & Perfit, M. 1990. Water contents, temperatures and diversity of the magmas of the catastrophic eruption of Nevado del Ruiz, Colombia, November 13, 1985. Journal of Volcanology and Geothermal Research, 41(1–4): 97–126. https://doi.org/10.1016/0377–0273(90)90085–T

Méndez, R.A. & Patiño, J.d.J. 1994. Estudio tefroestratigráfico de los volcanes del Complejo Machín–Cerro Bravo. Ingeominas, unpublished report, 19 p, Manizales.

Monsalve, M.L. & Méndez, R.A. 1997. Geología superficial del área geotérmica de Nereidas, Nevado del Ruiz. Ingeominas, unpublished report, 20 p. Manizales.

Mora, H., Diederix H., Bohórquez O., Peláez J.R., Martínez G., Cardozo S., Cardona L., Corchuelo Y., Lizarazo S., Ramírez J., Giraldo L., Díaz, F., Moreno R. & Álvarez C.E. 2016. Mapa de Velocidades Geodésicas Horizontales de Colombia. VII Taller Aplicaciones Científicas GNSS en Colombia, Póster. Bogotá.

Murcia, H.F., Borrero, C.A., Pardo, N., Alvarado, G.E., Arnosio, M. & Scolamacchia, T. 2013. Depósitos volcaniclásticos: Términos y conceptos para una clasificación en español. Revista Geológica de América Central, 48:15–39.

Murcia, H., Borrero, C. & Németh, K. 2017. Campos volcánicos monogenéticos asociados a la cadena volcánica de la parte media de la cordillera Central de Colombia. XVI Congreso Colombiano de Geología. Memoirs, p. 2019–2021. Santa Marta.

Naranjo, J.L. & Ríos, P.A. 1989. Geología de Manizales y sus alrededores y su influencia en los riesgos geológicos. Revista Universidad de Caldas, 10(1–3): 1–3.

Nelson, H.W. 1957. Contribution to the geology of the Central and Western Cordillera of Colombia in the sector between Ibagué and Cali. Leidse Geologische Mededelingen, 22: 1–75. Leiden, the Netherlands.

Pardo, N., Pulgarín, B.A. & Betancourt, V. 2016. Avances en el conocimiento geológico sobre el Complejo Volcánico Doña Juana: Integración del análisis de litofacies, estratigrafía, geocronología y petrología. Servicio Geológico Colombiano, unpublished report, 267 p. Bogotá.

Pardo, N., Pulgarín, B.A., Betancourt, V., Lucchi, F. & Valencia L.J. 2019. Facing geological mapping at low–latitude volcanoes: The Doña Juana Volcanic Complex study–case, SW Colombia. Journal of Volcanology and Geothermal Research, 385: 46–67. https://doi.org/10.1016/j.jvolgeores.2018.04.016

Pierson, T.C., Janda, R.J., Thouret, J.C. & Borrero, C.A. 1990. Perturbation and melting of snow and ice by the 13 November 1985 eruption of Nevado del Ruiz, Colombia, and consequent mobilization, flow and deposition of lahars. Journal of Volcanology and Geothermal Research, 41(1–4): 17–66. https://doi.org/10.1016/0377–0273(90)90082–Q

Pujadas, A., Brusi, D. & Pedrinaci, E. 1999. ¡Los volcanes han cambiado! Nuevos enfoques de terminología volcánica. In: Universidad de Girona (editor), Enseñanza de las ciencias de la Tierra., 7.3: p. 200–209. Girona, Spain.

Pulgarín–Alzate, B.A., Tamayo–Alzate, M., Correa–Tamayo, A.M., Ceballos–Hernández, J.A., Cruz–Toro, Y.P. & Méndez–Fajury, R. 2020. Stratigraphy and geological evolution of the Paramillo de Santa Rosa Volcanic Complex and its Pleistocene to Holocene eruptive history. In: Gómez, J. & Pinilla–Pachon, A.O. (editors), The Geology of Colombia, Volume 4 Quaternary. Servicio Geológico Colombiano, Publicaciones Geológicas Especiales 38, p. 197–226. Bogotá. https://doi.org/10.32685/pub.esp.38.2019.05

Restrepo–Pace, P.A. 1992. Petrotectonic characterization of the Central Andean Terrane, Colombia. Journal of South American Earth Sciences, 5(1): 97–116. https://doi.org/10.1016/0895–9811(92)90062–4

Rudnick, R.L. & Gao, S. 2003. Composition of the continental crust. In: Holland, H.D. & Turekian, K.K. (editors), Treatise on Geochemistry. Elsevier Ltd., p. 1–64. Amsterdam, The Netherlands. https://doi.org/10.1016/B0–08–043751–6/03016–4

Salvador, A. 1994. International Stratigraphic Guide: A guide to stratigraphic classification, terminology, and procedure. 2nd edition. The International Union of Geological Sciences & The Geological Society of America, 214 p. Boulder, USA. https://doi.org/10.1130/9780813774022

Schaefer, S.J. 1995. Nevado del Ruiz Volcano, Colombia: Magmatic system and evolution. Doctorade thesis, Arizona State University. 147p. Phoenix, USA.

Sigurdsson, H., Carey, S., Palais, J.M. & Devine, J. 1990. Pre–eruption compositional gradients and mixing of andesite and dacite magma erupted from Nevado del Ruiz Volcano, Colombia in 1985. Journal of Volcanology and Geothermal Research, 41(1–4): 127–151. https://doi.org/10.1016/0377–0273(90)90086–U

Sigurdsson, H., Houghton, B., McNutt, S.R., Rymer, H. & Stix, J., editors. 2000. Encyclopedia of Volcanoes. Academic Press, 417 p. San Diego, USA.

Thouret, J.C. 1988. La Cordillère Centrale des Andes de Colombie et ses bordures: Morphogenèse Plio – Quaternaire et dynamique actuelle et récente d'une cordillère volcanique englacée. Doctorade thesis, Université Joseph Fourier, 327 p. Grenoble, France.

Thouret, J.C., Murcia, L.A., Salinas, R. & Vatin–Pérignon, N. 1985. Cronoestratigrafía mediante dataciones K/Ar y ^{14}C de los volcanes compuestos del Complejo Ruiz–Tolima y aspectos volcano–estructurales del Nevado del Ruiz, cordillera Central, Colombia. VI Congreso Latinoamericano de Geología. Memoirs, p. 387–452. Bogotá.

Thouret, J.C., Cantagrel, J.M., Salinas, R. & Murcia, A. 1990. Quaternary eruptive history of Nevado del Ruiz, Colombia. Journal of Volcanology and Geothermal Research, 41(1–4): 225–251. https://doi.org/10.1016/0377–0273(90)90090–3

Toro, L.M., Borrero, C.A. & Ayala, L.F. 2010. Petrografía y geoquímica de las rocas ancestrales del Volcán Nevado del Ruiz. Boletín de Geología, 32(1): 95–105.

Toro, R.A. & Osorio, J.A. 2005. Determinación de los tensores de esfuerzos actuales para el segmento norte de los Andes calculados a partir de mecanismos focales de sismos mayores. Boletín de Geología, 27(1): 13–24.

Trenkamp, R., Kellogg, J.N., Freymueller, J.T. & Mora, H. 2002. Wide plate margin deformation, southern Central America and northwestern South America, CASA GPS observations. Journal of South American Earth Sciences, 15(2): 157–171. https://doi.org/10.1016/S0895–9811(02)00018–4

Vargas, C.A. & Mann, P. 2013. Tearing and breaking off of subducted slabs as the result of collision of the Panama Arc–indenter with northwestern South America. Bulletin of the Seismological Society of America, 103(3): 2025–2046. https://doi.org/10.1785/0120120328

Vatin–Pérignon, N., Goemans, P., Oliver, R.A. & Parra, E. 1990. Evaluation of magmatic processes for the products of the Nevado del Ruiz Volcano, Colombia, from geochemical and petrological data. Journal of Volcanology and Geothermal Research, 41(1–4): 153–176. https://doi.org/10.1016/0377–0273(90)90087–V

Vesga, C.J. & Barrero, D. 1978. Edades K/Ar en rocas ígneas y metamórficas de la cordillera Central de Colombia y su implicación geológica. II Congreso Colombiano de Geología. Abstracts, p. 19. Bogotá.

Villagómez, D.R. 2010. Thermochronology, geochronology and geochemistry of the Western and Central Cordilleras and Sierra Nevada de Santa Marta, Colombia: The tectonic evolution of NW South America. Doctorade thesis, University of Geneva, 143 p. Geneva. https://doi.org/10.13097/archive–ouverte/unige:14270

Young, R.H. 1991. Eruption dynamics and petrology of the most recent eruptions of Nevado del Ruiz Volcano, Colombia, South America. Master thesis, Louisiana State University, 121p. Baton Rouge, USA.

Explanation of Acronyms, Abbreviations, and Symbols:

ASTER	Advanced Spaceborne Thermal Emission and Reflection Radiometer
DEM	Digital elevation model
FEPR	First eruptive period Ruiz
FEPR–LD	First eruptive period Ruiz lava flows
GeoRED	Geodesia: Red de Estudios de Deformación
HFSEs	High field strength elements
HREEs	Heavy rare earth elements
ICP–MS	Inductively coupled plasma mass spectrometry
IEPR	Intermediate eruptive period Ruiz
IGAC	Instituto Geográfico Agustín Codazzi
IVACEI	International Association of Volcanology and Chemistry of the Earth's Interior
JAXA	Japan Aerospace Exploration Agency
LFSEs	Low field strength elements
LILEs	Large–ion lithophile elements
LREEs	Light rare earth elements
MREEs	Middle rare–earth elements
NASA	National Aeronautics and Space Administration
NRV	Nevado del Ruiz Volcano
NRVC	Nevado del Ruiz Volcanic Complex
OVSM	Observatorio Vulcanológico y Sismológico de Manizales
PRE–LD	Pre–Ruiz eruptive period lava flows
PDC	Pyroclastic density currents
RC–EU	Río Claro eruptive unit
REEs	Rare earth elements
SCVTP	San Diego–Cerro Machín Volcano Tectonic Province
SEPR	Second eruptive period Ruiz
SEPR–LD	Second eruptive period Ruiz lava flows
SGC	Servicio Geológico Colombiano
STRM	Shuttle Radar Topography Mission
TFS	Villamaría–Termales Fault System
UAVSAR	Uninhabited aerial vehicle synthetic aperture radar
VEI	Volcanic Explosivity Index

Authors' Biographical Notes

Julián Andrés CEBALLOS–HERNÁNDEZ is a geologist who graduated from the Universidad de Caldas (2007) and has worked at the Observatorio Vulcanológico y Sismológico de Manizales of the Servicio Geológico Colombiano since 2012. He was the technical coordinator for the "Volcanic Hazard Map of NRV, Third Version". He has participated in geological mapping and research in the Nevado del Ruiz, Paramillo de Santa Rosa, and Galeras Volcanic Complexes and has worked with computational simulations of lahars from the Nevado del Ruiz, Galeras, Chiles, and Cerro Negro Volcanoes. He also has experience working on socialization–communication projects within the framework of volcanic risk management.

Lilly Maritza MARTÍNEZ–TABARES is a geologist and master in Earth sciences candidate at Universidad de Caldas. She has worked at the Servicio Geológico Colombiano since 2010 and participated in the Grupo de Geología de Volcanes from 2010 to 2013, where she participated in the projects "Geology and eruptive history of the Sotará–Sucubún Volcanic Region" and "Geology and stratigraphy of the NRVC". Since 2014, she has worked on the "Volcanic Hazard Map of NRV, Third Version" project. Currently, she is working on the "Actualization of Volcanic Hazard Map of Cerro Bravo Volcano" project.

Luis Gerónimo VALENCIA–RAMÍREZ is a geologist who focuses mainly on volcanology and metallic mineral exploration. In 2007, he participated in the Neogene and Quaternary Vulcanism of the Colombian SW project. For 3 years, he worked on explorations of base minerals for companies such as AngloGold Ashanti and Minera Quinchía. Between 2012 and 2017, he carried out research with the Grupo de Geología de Volcanes of the Servicio Geológico Colombiano, where he mainly studied the geomorphology of volcanic zones and their relationships with glacial periods. He also participated in geological studies on the Nevado del Ruiz and Paramillo de Santa Rosa Volcanoes.

Bernardo Alonso PULGARÍN–ALZATE is a geologist engineer (1987) with an MS in volcanology (2000) from the Universidad Nacional Autónoma de México. His professional job has been focused on understanding volcanic geology–stratigraphy and the eruptive histories of volcanoes as well as in the searching for good practices for standardization of volcanoes geological maps. He also has experience working with volcanic hazards, glacier retreat, and socialization and communication with communities that live under threat of geological hazards. He has worked for the Servicio Geológico Colombiano (SGC) at the Observatorio Vulcanológico y Sismológico de Popayán for 32 years. He has carried out geological work and research on several Colombian volcanoes (Puracé, Los Coconucos volcanic chain, Nevado de Santa Isabel, Nevado del Huila, Doña Juana, Sotará, Sucubún, Nevado del Ruiz, Paramillo de Santa Rosa, and Galeras). He is currently the coordinator of the Grupo de Geología de Volcanes of the SGC.

Ana María CORREA–TAMAYO is a geologist (1992) with a PhD in geology (2009) from the Universidad Complutense de Madrid. Her professional job has been focused on volcanic cartography and stratigraphy, petrographic and geochemical studies of volcanoes, and their eruptive history. She has been working at the Servicio Geológico Colombiano (SGC) for 10 years. She has performed geological work and research on several Colombian volcanoes (Nevado del Huila, Azufral, Paramillo de Santa Rosa, Doña Juana, Nevado del Ruiz, and Sotará). She is currently a member of the Grupo de Geología de Volcanes of the SGC.

Blanca Liliana NARVÁEZ–MARULANDA is a geologist and former researcher at the Servicio Geológico Colombiano, with four years of experience in state–level projects that assessed exposed areas and probable loss and damage in mountain environments, specifically in volcanic risk scenarios in the Colombian Andes. She is a MS candidate in geography of environmental risks and human security offered by Bonn Universität and the United Nations University, Bonn, Germany. She is conducting ongoing research related to adaptation to climate change and disaster risk reduction based on ecosystems in Latin America. Currently, she is a student assistant in the Environmental Human Security section at the United Nations University in the Global Mountain Safeguard Research (GLOMOS) initiative.